MRI-based Brain Tumor detection using Deep Learning Techniques

By

Ammar Ahmed Qureshi

Fall-2021-MS-EE-TCN 360995 SEECS

Department of Electrical Engineering

School of Electrical Engineering & Computer Science (SEECS)

National University of Sciences and Technology (NUST)

Islamabad, Pakistan.

(2024)

MRI-based Brain Tumor detection using Deep Learning Techniques

By

Ammar Ahmed Qureshi

Fall-2021-MS-EE-TCN 360995 SEECS

A thesis submitted to the National University of Sciences and Technology, Islamabad,

in partial fulfillment of the requirements for the degree of

Master of Science in
Electrical Engineering

Supervisor

Dr. Wajid Mumtaz

School of Electrical Engineering & Computer Science (SEECS)

National University of Sciences and Technology (NUST)

Islamabad, Pakistan

(2024)

THESIS ACCEPTANCE CERTIFICATE

Certified that final copy of MS/MPhil thesis entitled "MRI-based Brain Tumor detection using Deep Learning Techinques " written by Ammar Ahmed Qureshi, (Registration No 360995), of SEECS has been vetted by the undersigned, found complete in all respects as per NUST Statutes/Regulations, is free of plagiarism, errors and mistakes and is accepted as partial fulfillment for award of MS/M Phil degree. It is further certified that necessary amendments as pointed out by GEC members of the scholar have also been incorporated in the said thesis.

Signature: _____

Name of Advisor: ___Dr. Wajid Mumtaz___

Date: _____27-Feb-2024_____

HoD/Associate Dean: _____

Date: _____26/3/24_____

Signature (Dean/Principal): _____
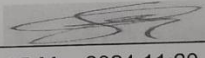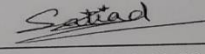
Date: ___27 – May – 2024___

Dr. Muhammad Ajmal
Principal
NUST School of Electrical
Engg & Computer Science
H-12, Islamabad

National University of Sciences & Technology
MASTER THESIS WORK

We hereby recommend that the dissertation prepared under our supervision by: (Student Name & Reg. #)___Ammar Ahmed Qureshi [360995]___

Titled: MRI-based Brain Tumor detection using Deep Learning Techinques

be accepted in partial fulfillment of the requirements for the award of ___Master of Science (Electrical Engineering)_____degree.

Examination Committee Members

1. Name: Salman Abdul Ghafoor_____   Signature:_____
   25-Mar-2024 11:20 AM

2. Name: Sajjad Hussain_____   Signature:_____
   25-Mar-2024 11:20 AM

Supervisor's name: Wajid Mumtaz_____   Signature:_____
   25-Mar-2024 11:27 AM

_____   _____
HoD/Associate Dean   26/3/24
                                        Date

COUNTERSINGED

                                        Dr. Muhammad Ajmal
                                        Principal
                                        NUST School of Electrical
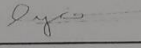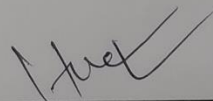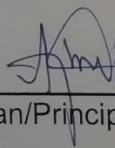   Engg & Computer Science
___27—May—2024___   _____ Islamabad
     Date   Dean/Principal

Certificate of Approval

This is to certify that the research work presented in this thesis, entitled "**MRI-based Brain Tumor detection using Deep Learning Techniques** " was conducted by **Ammar Ahmed Qureshi** under the supervision of Dr. Wajid Mumtaz.

No part of this thesis has been submitted anywhere else for any other degree. This thesis is submitted to the Department of Electrical Engineering, School of Electrical Engineering and Computer Science (SEECS) in partial fulfillment of the requirements for the degree of Master of Science in the Field of Electrical Engineering, Department of Electrical Engineering, National University of Sciences and Technology, Islamabad.

Student Name: **Ammar Ahmed Qureshi**   Signature:

Examination Committee:

    a) External Examiner 1: Name: **Dr. Sajjad Hussain**   Signature: _____
    (Designation & Office Address)

    b) External Examiner 2: Name: **Dr. Salman Abdul Ghafoor** Signature: _____
    (Designation & Office Address)

Supervisor Name: **Dr. Wajid Mumtaz**   Signature: _____

Name of Dean/HOD: **Dr. Salman Abdul Ghafoor**   Signature: _____

AUTHOR'S DECLARATION

I Ammar Ahmed Qureshi hereby state that my MS thesis titled "**MRI-based Brain Tumor detection using Deep Learning Techniques**" is my own work and has not been submitted previously by me for taking any degree from National University of Sciences and Technology, Islamabad or anywhere else in the country/ world.

At any time if my statement is found to be incorrect even after I graduate, the university has the right to withdraw my MS degree.

Author Name: **Ammar Ahmed Qureshi**

Signature: _____

PLAGIARISM UNDERTAKING

I solemnly declare that the research work presented in the thesis titled "**MRI-based Brain Tumor detection using Deep Learning Techniques**" is solely my research work with no significant contribution from any other person. Small contribution/ help wherever taken has been duly acknowledged and that complete thesis has been written by me.

I understand the zero-tolerance policy of the HEC and the National University of Sciences and Technology (NUST), Islamabad towards plagiarism. Therefore, I as an author of the above-titled thesis declare that no portion of my thesis has been plagiarized and any material used as reference is properly referred/cited.

I undertake that if I am found guilty of any formal plagiarism in the above-titled thesis even after the award of my MS degree, the University reserves the right to withdraw/revoke my MS degree and that HEC and NUST, Islamabad has the right to publish my name on the HEC/University website on which names of students are placed who submitted plagiarized thesis.

Student Signature:

Name: Ammar Ahmed Qureshi

DEDICATION

I am humbled and honored to dedicate this thesis book to the most important people in my life, my beloved family. Throughout this challenging yet rewarding journey, your unwavering support, love, and understanding have been my constant pillars of strength. From the early days of my academic pursuits to the late nights of writing and research, you have been there, cheering me on and believing in my abilities even when I doubted myself. Your sacrifices, patience, and encouragement have been the fuel that kept me going, and I am forever grateful for everything you have done.

To my esteemed supervisor **Dr. Wajid Mumtaz**, I extend my deepest gratitude for your exceptional guidance and mentorship. Your profound knowledge, passion for research, and dedication to your field have shaped the outcome of this thesis in ways I could not have imagined. Your constructive feedback, patience, and unwavering belief in my potential have inspired me to strive for excellence. Working under your guidance has been an honor and a privilege, and I am proud to dedicate this thesis to you as a token of my appreciation.

To my esteemed co-supervisors **Dr. Sajjad Hussain**, and **Dr. Salman Abdul Ghafoor**, I am immensely grateful for your invaluable contributions to this work. Your expertise and insights have enriched the research and broadened my perspective. Your unwavering support and encouragement have motivated me to delve deeper into my studies and explore new avenues of knowledge. I am indebted to each of you for your mentorship and dedication to my academic growth, and I proudly dedicate this thesis to all of my co-supervisors.

Acknowledgment

Glory be to Allah (S.W.A), the Creator, the Sustainer of the Universe. Who only has the power to honor whom He pleases, and to abase whom He pleases. Verily no one can do anything without His will. From the day I came to NUST till the day of my departure, He was the only one Who blessed me, opened ways for me, and showed me the path of success. There is nothing that can payback for his bounties throughout my research period to complete it successfully.

Ammar Ahmed Qureshi

Contents

List of Figures

List of Tables

List of Abbreviations

Abbreviation	Explanation
WHO	World Health Organization
CNN	Convolutional Neural Network
CNS	Central Nervous System
MRI	Magnetic Resonance Imaging
DL	Deep Learning
AI	Artificial Intelligence
YOLO	You Only Look Once
CAD	Computer Aided Diagnosis
COCO	Common Objects in Context
TL	Transfer Learning
VGG	Visual Geometry Group
SVM	Support Vector Machines
R-CNN	Region-Based Convolutional Neural Network
E-ELAN	Extended Efficient Layer Aggregation Network
mAP	Mean Average Precision
PR	Precision Recall
RC	Recall
IoU	Intersection Over Union

Abstract

Automated brain tumor detection is vital for early identification of tumors, enabling timely medical intervention and improving overall tumor detection outcomes for patients. This study proposes a novel approach that utilizes the advanced DL technique YOLOv7 object detection framework, to achieve precise and real-time identification of brain tumors using MRI images. The manual review method is laborious and requires specialized knowledge to prevent human errors. Hence, the necessity for an automated brain tumor detection system arises to facilitate timely diagnosis of the disease. The YOLOv7 model underwent training using a dataset of 7023 MRI images that were pre-processed and labeled. An effective collection of characteristics for brain tumor identification was created by employing transfer learning and utilizing pre-trained weights from the MSCOCO dataset. The model achieved a mean average precision of 81.7% for glioma, 98.6% for meningioma, 98.1% for pituitary, and 98.6% for brain without a tumor. The results demonstrated a superior performance of the YOLO detection models compared to prior versions and other studies that employed bounding box detections. The mean average precision achieved was 93.14%, with a precision of 90.34%, recall of 88.58%, and F1-Score of 89.45%. Based on the results, it has been determined that the YOLOv7 model is capable of effectively and automatically detecting brain tumors at a fast pace by utilizing appropriate fine-tuning and transfer learning techniques. The primary purpose of the research is to assist healthcare practitioners in identifying brain tumors by utilizing imaging techniques.

Chapter 1

Introduction and Motivation

1. Introduction

The CNS, which encompasses the complexities of the brain and spinal cord, continues to be an enigmatic domain about its capabilities. The emergence of brain tumors in this complex system poses a significant and difficult problem, marked by the growth of abnormal cells that grow uncontrollably. This can result in premature death or long-lasting consequences. The escalating prevalence of brain tumors, both primary and secondary, has emerged as a critical health concern globally. As an increasing number of individuals are diagnosed with brain tumors, early detection becomes imperative for effective intervention.

Understanding the gravity of the issue, recent studies reveal that nearly 70,000 people in the US suffer from brain tumors, making it the 10th most common tumor in the country [1]. The tumors have a significant impact on patients that goes beyond the physical aspect. Patients with brain tumors encounter the issue of the MRI machine's inability to accurately identify and categorize the tumor. This can result in various physical complications, ranging from mobility problems to sensory impairments, and even severe disabilities. Classification of these tumors into distinct types, including glioma, meningioma, and pituitary tumors, further emphasizes the intricate nature of brain pathology [2]. Primary brain tumors, including Gliomas, Meningiomas, and Pituitary, account for 1.4% of all cancer occurrences in the US. There are approximately 20,500 new cases and 12,500 deaths attributed to these tumors [3]. Cerebral glioma is a highly concerning tumor that arises from the glial cells in the brain. Its aggressive nature characterizes it and affects around 14,000 Americans per year, with a growing incidence rate. The severity of Gliomas is underscored by their classification as grade IV tumors by the WHO, denoting their malignant and deadly nature. In contrast, pituitary tumors, slow-growing entities within the pituitary gland, present a less aggressive profile compared to Gliomas In contrast to its contemporaries, pituitary tumors have a minimal risk of malignancy and rarely spread forcefully to other body areas. Meningiomas, with

an incidence rate of six to eight cases per 100,000 individuals annually, can arise from the meningeal coverings of the brain or the meninges of the spine. While benign meningiomas and pituitary tumors may not necessitate immediate medical attention, their accelerated progression can lead to symptoms such as recurrent morning headaches, visual impairment, or seizures.

The imperative to mitigate untimely deaths underscores the necessity for proper diagnosis and treatment of brain tumors, regardless of their degree or severity. Patients experiencing symptoms associated with these tumors are advised to undergo non-invasive diagnostic methods, such as MRI, for immediate detection. However, the analysis of MRI scan results demands thorough observation and a high level of proficiency, often posing a challenge in healthcare facilities lacking the necessary competence. The urgency of timely diagnosis is underscored by the potentially life-threatening consequences of untreated cases, with approximately 5,230 children under the age of 20 also expected to be diagnosed with central nervous system tumors in 2023. In response to the complexities associated with brain tumor diagnosis, there is a growing interest in automated Computer-Aided Diagnosis (CAD) systems. These systems aim to provide rapid and accurate detection, thereby assisting medical experts in improving patient outcomes and quality of life [3]. DL is an AI technique that relies on training to create many layers of computation. These layers are designed to instruct the development of machine representations of input at various levels. The utilization of this methodology has greatly propelled the development of numerous technologies, encompassing but not restricted to speech recognition and object identification in a wide range of fields. The training procedure in deep learning can manifest as either supervised or unsupervised learning. DL can transform incoming data at several levels into a more abstract and organized representation. In the case of tumor recognition applications, the initial input data usually consists of a matrix of pixels. The primary layer of the representation abstracts the pixel data and encodes it in a manner that enhances the identification of tumor boundaries. Following this, the subsequent layer encodes information about the arrangement of tumor edges, whereas the third layer of representation encodes the depiction of circular patterns. In essence, the process within deep learning autonomously extracts features from the data and organizes them to fit the relevant context, enabling the recognition of complex patterns, such as tumor structures. We have chosen to examine the efficacy of the YOLO object detection framework in accurately detecting and classifying brain tumors. YOLO, a neural network-based framework for object recognition, has gained significant popularity in recent years. Several scientific papers have proposed YOLO-based

object detection models. Interestingly, there hasn't been much research done on this architecture to detect brain tumors. The aim of this study is to create a sophisticated deep-learning model using the most recent versions of the YOLO framework. This model will be used to accurately classify and detect brain tumors. The ultimate goal is to develop an automated system for real-time brain tumor detection. The exploration of YOLOv7 in the identification of brain tumors in MRIs has not been extensively studied in current academic literature. Therefore, there is a need for further inquiry to assess its overall precision. This solution may provide greater flexibility to medical professionals and smaller healthcare institutions, allowing them to diagnose brain tumors more quickly.

1.1 Brain Tumor Types

Medical experts have observed a vast range of brain tumors with varying effects and grades. Some common brain tumors include the following:

Glioma: Glioma is a malignancy originating from the glial cells, which are the nerve cells that surround the brain and spinal cord. Medical studies have identified three prevalent forms of gliomas. Astrocytoma originates in the glial cells that have a star-like shape. Astrocytoma, anaplastic astrocytoma, and glioblastomas are the three main types of these malignancies. A subset of glial cells called oligodendrocytes are the progenitors of oligodendrocytes. The anaplastic oligoastrocytoma, oligodendroglioma, and other gliomas that originate from microglia, satellite cells, and Schwann cells can be further categorized [37]**.**
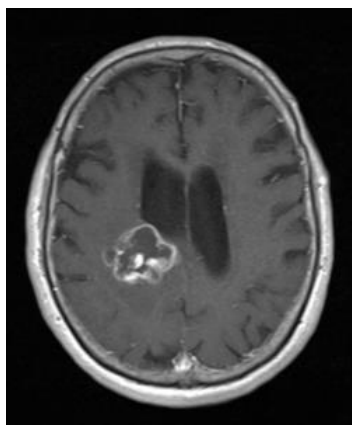
Figure 1.1: Glioma Brain Tumor

Meningioma: Meningioma [38] tumors originate from the meninges, the protective membranes that enclose the brain within the skull. These tumors exhibit a sluggish rate of growth and are

typically classified as benign. Occasionally, meningioma tumors might undergo malignant changes.
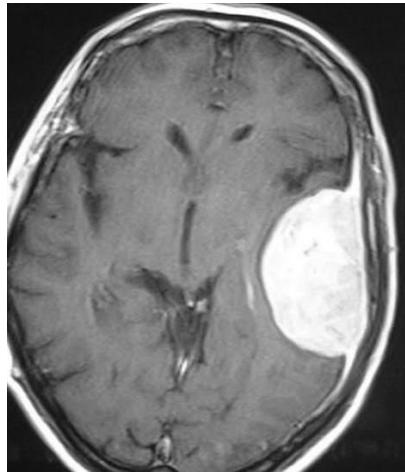
Figure 1.2: Meningioma Brain Tumor

Pituitary adenomas: Pituitary adenomas [39] are neoplasms with a slow growth rate forms in the pituitary gland, at the base of the brain. This form of tumor exerts an influence on both the pituitary hormones and the entire body.
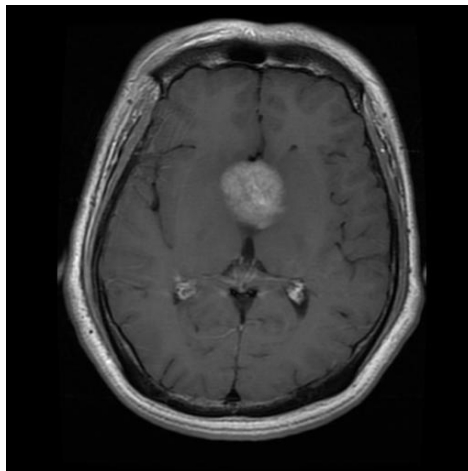
Figure 1.3: Pituitary Brain Tumor

1.2 Symptoms of Brain Tumor

The symptoms of brain tumors might differ depending on the specific type and grade of the tumor. Nevertheless, certain generic signs are more prevalent. The symptoms of brain tumors have been categorized into general and specific groups [40].

Headaches: They can be intense and exacerbate, especially in the early hours or during physical activity.

Seizures: Seizures are abrupt, uncontrollable, and involuntary movements caused by disruptions in the brain's electrical activity. These seizures are classified as myoclonic and tonic-clonic seizures. Myoclonic seizures are characterized by individual muscular spasms, sudden movements, or convulsions. However, tonic-colonic seizures involve the complete loss of awareness, muscular tone, and control over urination.

Sensory Issues: Alterations in perception may occur, such as hearing, visual, or olfactory impairment, without loss of consciousness. Also, vomiting can occur many times in a day.

Fatigue: Severe fatigue can manifest as insomnia, sadness, memory loss, vertigo, and other symptoms. Conversely, specific signs are linked to the type, severity, and area of the brain tumor: Challenges in forming assessments, engaging in decision-making, or experiencing a decline in motivation are associated with the frontal lobe of the cerebrum.

Visual impairment, whether whole or partial, is specifically located in the occipital lobe of the cerebrum. The pituitary gland is linked to lactation, irregular menstruation periods in women, and growth-related issues.

Diplopia, dysphagia, and paresthesia are characteristic of brainstem involvement.

1.3 Motivation

One of the primary motivating factors for this research endeavor is the pressing necessity to advance the detection of brain tumors, which is a major obstacle in the medical field where timely and accurate diagnosis is important. Conventional approaches to diagnosing brain tumors sometimes include a labor-intensive, subjective, and error-prone manual examination. The aim of this work is to improve the efficiency and precision of brain tumor detection by employing various advanced deep-learning models, such as ResNet50, ResNet18, Inception v3, AlexNet, and others. The work specifically involves utilizing YOLOv7 for accurate bounding box prediction, which is

a feature not commonly offered by other models that exclusively focus on image classification. If implemented successfully, it could result in accelerated treatments, enhanced patient outcomes, and decreased need on manual analysis. In conclusion, people who are dealing with brain tumors have the potential to greatly gain from the results of this research, which will contribute to developments in the field of medical imaging analysis. The prospective ramifications of this research are significant, as it offers the opportunity to develop effective and dependable instruments for healthcare practitioners, therefore driving advancements in medical diagnostics.

1.4 Thesis Objectives

This work provides the following significant contributions:

1. Collection of a dataset consisting of a wide range of MRI images illustrating different categories of brain tumors obtained from the hospital. The dataset is a valuable asset for training and evaluating the suggested model.

2. To ensure the exactness and correctness of the model, the collected MRI images underwent meticulous annotation using the labelImg tool with the help of a medical expert.

3. The Yolov7 model is specifically designed and optimized to classify and detect brain tumors. This model has been designed to maximize the utilization of annotated data, offering a strong and reliable framework for precisely and quickly identifying brain tumors.

1.5 Thesis Structure

The rest of the thesis is organized as follows.

- In Chapter 2, we discuss state-of-the-art research on MRI based brain tumor detection using deep learning techniques. Their pros and cons are also discussed in this chapter. Methods, Online Resources, and research gaps in this domain are explained in this section.

- In Chapter 3, Transfer learning system explanation, the procedures we carried out for this thesis are discussed. This chapter discusses in detail the methodology of all the deep learning models we implemented in this thesis.

- In Chapter 4, brain tumor detection and classification is discussed using YOLOv7, the procedures we carried out for this thesis are discussed. This chapter discusses in detail the methodology of the YOLOv7 model, why it is used and what evaluation matrices were used to examine the results.

- In Chapter 5, we discuss the results computed for the study we carried out in our thesis. Their discussion and implementation are done in this chapter.

- In Chapter 6, the conclusion consists of a summary of findings, and the future of the thesis is discussed. The main contributions of this thesis as compared to other state of art research are also listed.

Chapter 2

Background Study

Extensive literature has been dedicated to the investigation of tumor identification using MRI. Radiologists find manual segmentation to be a time-consuming process, therefore, the use of automated or semi-automatic approaches is necessary to accurately locate tumors. Currently, the utilization of completely automated techniques for tumor classification based on MRI scans is prevalent in both clinical and research settings. These techniques can aid in the analysis of the tumor area and have experienced significant advancements in the past two decades. Hence, radiologists claim that computerized techniques, employing automated machine learning algorithms, can enhance their diagnostic capabilities. This chapter explores various deep learning methodologies, including conventional, semi-automated, manual, completely automatic, and model-based approaches. The study also covers strategies for extracting and selecting/reducing features, classifying data, and utilizing deep learning techniques. Recently, the combination of many DL models and sophisticated imaging methods has greatly improved CAD systems, especially in brain tumor classification. This advancement is being actively aided by magnetic resonance imaging, a vital component of modern medical techniques for the detection of brain tumors. This study of the literature explores the excellence achieved in the detection and classification of brain tumors, a field that continues to hold great importance in the medical world. The domain of brain tumor detection, classification, and segmentation has seen a rise in research efforts due to the increasing interest in this important medical field. With the yearly release of fresh datasets, the area has developed into a dynamic and busy study issue in recent decades. Magnetic Resonance Imaging is a vital diagnostic technique that is particularly useful for brain tumors. It eliminates the need for the laborious manual diagnosis process often performed by qualified radiologists. The use of automated methods represents a significant improvement in the speed at which brain tumors can be identified and categorized.

2. Literature Review

In [1], a dataset consisting of 1445 MRI images was utilized for training, with 310 pictures allocated for testing and another 310 images for validation. They used CNN and VGG-16 Architecture to classify 2 classes named tumor and no tumor. They achieved accuracies of 91.6 percent and 91.9 percent. In reference [2], The researchers employed pre-trained models and subsequently fine-tuned them to enhance the efficiency of the algorithms for classifying brain cancers in MRI data. They used pre-trained models namely Xception, Resnet50, inceptionV3, VGG16, and MobileNet. This work only classifies the brain tumor images instead of detecting the tumor in an MRI scan. In [3], the author used the YOLOv4-tiny model for the purpose of tumor detection. For this purpose, the MRI images of the brain were annotated first, to create ground truth for the training of the model. After that YOLOv4-tiny was applied. Transfer learning accelerates the training process by utilizing pre-trained weights obtained from the COCO dataset. The model achieved a good result. In [4],[5] the authors proposed a CNN with SVM and TL approach along with dimensionality reduction for the classification of tumor and non-tumor MRI images. They were able to successfully classify the MRI images. In reference [6], the author used KNN and SVM models for brain tumor classification in MRI scans. They used two different datasets containing MRI scans of tumorous and non-tumorous images. They were able to successfully classify the tumorous images. In [7], researchers introduced a hybrid approach for classifying brain tumors. This approach integrates features derived from the Gray Level Co-occurrence Matrix with a CNN. Four different datasets were used to evaluate the system. The Gl-Pt dataset achieved the best accuracy rate of 82.27%. In [8], [9], AlexNet convolutional neural network and an innovative architecture based on DL techniques have been proposed, combining DL methods with image classification. CNN with WOA and GWO were used to detect brain tumors. In reference [10], the author used Whale Harris Hawks optimization. The method introduces an optimization-centric approach to brain tumor diagnosis. The necessary characteristics, such as the tumor's dimensions, the local optical alignment pattern, and the statistical measures of mean, variance, and kurtosis, were obtained. The system has attained a precision level of 81.6%. In [11], [12], the author proposed a system utilizing CNN to identify and categorize brain cancers. The researchers successfully utilized a cascaded CNN algorithm to implement brain tumor segmentation. Additionally, they employed a fine-tuned VGG19 and

9

MobileNetV2 model to classify the tumors. Acceptable results were obtained by employing these methodologies. In reference [13], the author employed the VGG model for the purpose of detecting brain tumors. The model employs VGG16 as its foundational architecture to produce a feature map, which is subsequently utilized for the classification of brain tumors. The dataset utilized comprises 253 photos, with 155 of them depicting malignancy. In [14], the researchers proposed a new method for classifying brain tumors, which entailed combining a Recursive Extreme Learning Machine (RELM) with a hybrid feature extraction strategy. The brain tumor categorization was achieved using the recursive elimination least mean square method, yielding an accuracy of 94.23%. In reference [15], the author proposed a K-mean clustering approach for detecting brain tumors. The proposed model consists of 3 phases. In the 1st phase, brain images were segmented using the k-mean algorithm to generate clusters. The 2nd phase involves the selection of an appropriate cluster and in the last the brain tumor is determined. In the reference [16], [17], the author developed a system based on DL for the classification of brain tumors in MRI scans. The papers proposed employing LSTM and ResNet50. The studies seek to forecast the efficacy of the proposed model by utilizing the Kaggle dataset, comprising 3264 MRI scans. The presented models demonstrated a commendable tumor classification accuracy exceeding 90%. In reference [18], the author suggested brain tumor classifier, known as HDL2BTUMOR-CLASSIFIER, functions by utilizing three key layers. Collecting data, preprocessing layer, and the application layer. The model classifies glioma, meningioma, pituitary, and no-tumor, with an accuracy rate of 92.13%. In reference [19], researchers improved the CNN efficientNet-B0 model by incorporating additional layers to categorize the brain tumor. They employed a range of filters to improve the quality of the images. The suggested method surpassed the current cutting-edge CNN model and obtained extremely promising results. In [20], the author proposes the YOLOv5 framework and the FastAi DL library. The dataset included a total of 1,992 tumor MRI images, which encompassed both tumorous and non-tumorous images. The YOLOv5 attained an accuracy of 85.95%, however, the FastAi classification surpassed it by obtaining an accuracy of 95.78%. In [21], the author introduced a YOLOv2 methodology comprising four distinct stages: lesion enhancement, feature extraction, selection, localization, and segmentation. The proposed methodology has been successfully evaluated on the BRATS 2018, 2019, and 2020 datasets, demonstrating prediction scores of greater than 90% for tumor localization, segmentation, and classification. In [22], the study undertaken by the author provides empirical evidence supporting

the effectiveness of YOLO in the field of medical imaging. The study achieved superior results in skin lesion detection. The study's findings indicate that the combination of YOLO with the GrabCut segmentation technique exhibits promising capabilities as evidenced by the accuracy of 93.39 percent.

2.1 Problem Statement

In modern times, there has been a rise in the occurrence of brain tumors, and magnetic resonance imaging (MRI) scans are commonly used as a primary method for detecting abnormalities in brain tissue. The early detection of brain tumors can have a substantial impact on the variety of treatment choices available as well as the likelihood of survival. Tumors must be accurately identified and classified in order to determine the best course of treatment, which may include chemotherapy, surgery, radiation therapy, or a mix of these approaches. However, the challenges related to tumor segmentation and classification in medical picture applications primarily arise from the requirement to handle large amounts of data. Difficulties arise in these activities because of restrictions such as artifacts caused by a limited acquisition time and patient mobility, as well as the indistinct borders of soft tissue, which further complicate the procedure. Tumors exhibit a diverse array of forms, sizes, and imaging intensities, underscoring the importance of accurate segmentation to enhance the precision and efficacy of classification. Each model possesses intrinsic constraints. Several scholars in the academic domain have proposed diverse classification techniques for the identification and categorization of brain tumors. Nevertheless, there are constraints in dealing with intricate computations, prolonged processing durations, and the precision of identifying brain tumors and their distinct manifestations in this particular scenario.

Table 2.1: Literature Review of MRI Brain Tumor Detection and Classification

Year	Ref.	Paper Title	Models	Accuracy
2020	[1]	Brain tumor detection using deep learning models	CNN VGG16	91.6% 91.9%
2023	[9]	Innovative brain tumor detection using optimized deep-learning techniques	CNN ACO BCO GLCM	93.9% 94.2% 94.7% 95.9%
2022	[16]	Enhanced Watershed Segmentation Algorithm-Based Modified ResNet50 Model for Brain Tumor Detection	Modified ResNet50 watershed technique, and transfer learning approach.	90%
2022	[36]	Data Augmentation and Transfer Learning for Brain Tumor Detection in Magnetic Resonance Imaging	PCA-based augmentation achieved with the ResNet50 network	92.34
2022	[4]	Brain Tumor Detection Using Transfer Learning with Dimensionality Reduction Method	CNN with a transfer learning approach along with the dimensionality reduction method EfficientNet-B7 model.	80%

Chapter 3

Brain Tumor Classification Using Transfer Learning Based Models

3. Introduction

Following our methodology, we gathered a dataset of brain MRI scans obtained from both Kaggle and HMC Peshawar. This section offers a comprehensive description of the manner in which our work is carried out, which is broken down into distinct phases that include the collection of data, the preparation of the dataset, the explanation of the proposed model, the training of the model, and ultimately the evaluation of its capability. Within the scope of this part, we will investigate three essential aspects: the preparation of the dataset, the description of the dataset, and modeling transfer learning. We provide a comprehensive elucidation of the dataset that was employed, shedding insight into its composition as well as its characteristics. We analyze the techniques and procedures used to carefully select and prepare the data in order to enhance the efficiency of the model. In addition, we clarify the transfer learning models that were used, highlighting their effectiveness in utilizing pre-trained models for various tasks and demonstrating the techniques taken to do this. Figure 3.1 provides a comprehensive summary of the entire effort.
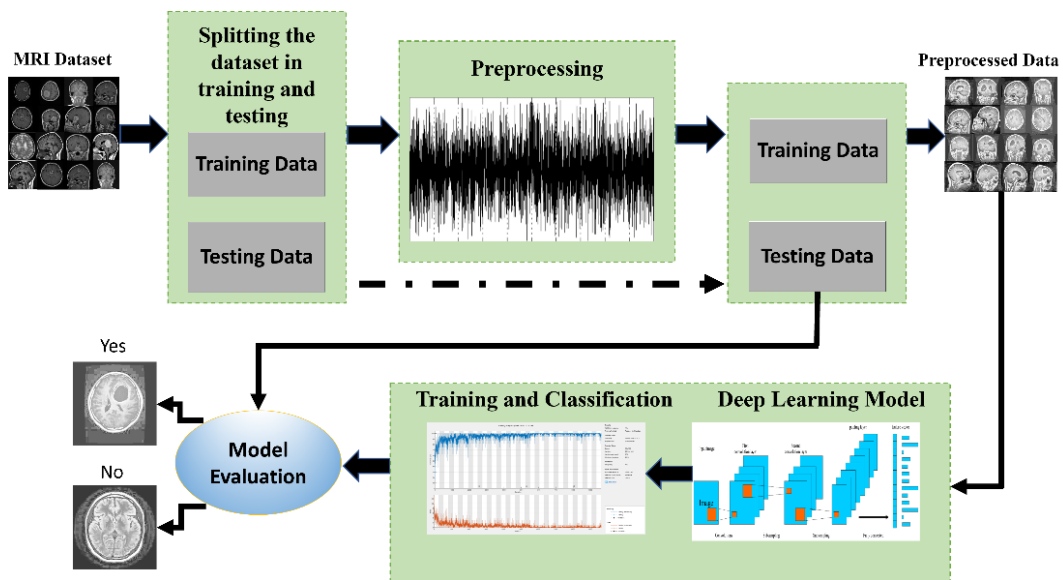

Figure 3.1: Overview of the Study
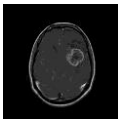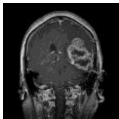
13

3.1   Dataset Description
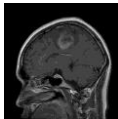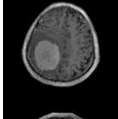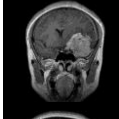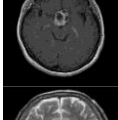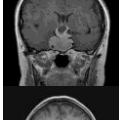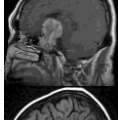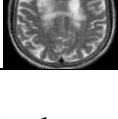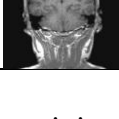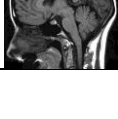
A comprehensive dataset consisting of brain scans from multiple imaging modalities, including MRI, has been chosen for the training of the YOLOv7 model. The dataset has been carefully selected to provide exposure to a wide variety of clinical situations, including cases of pituitary, meningioma, glioma, and no tumor. The dataset was obtained from Kagle and Hayatabad Medical Complex Peshawar. Table 3.1 describes the specifications of the dataset, consisting of 1594 healthy brain samples, 1321 glioma, 1339 meningioma, and 1457 pituitary brain tumor samples.

Table 3.1: MRI Brain Tumor Dataset Specifications

Class	Axial	Coronal	Sagittal	Total
Glioma	473	496	352	1321
Meningioma	441	422	476	1339
Pituitary	423	521	513	1457
No Tumor	103	1400	91	1594

Table 3.2 displays representative samples from each class in the dataset, showcasing multiple viewpoints, including axial, coronal, and sagittal. These samples offer a thorough visual depiction of various instances within the dataset, having been meticulously pre-sorted and checked by an expert radiologist.

Table 3.2: MRI Barin Tumor Samples

Class	Axial	Coronal	Sagittal
Glioma			
Meningioma			
Pituitary			
No Tumor			

As illustrated in Table 3.3 the dataset comprises training and testing sets corresponding to distinct classes of brain tumors. By employing a sufficient amount of learnable patterns from the training

data, this method can help in determining how effectively the model can identify brain tumors in the unknown data.

Table 3.3: Training and Testing Data

Class	Train Data	Test Data
Glioma	1321	327
Meningioma	1339	306
Pituitary	1457	300
No Tumor	1594	405

3.2 Image Preprocessing

Various approaches are employed in dataset preparation of brain MRI image preprocessing to enhance image quality and enable a more comprehensive analysis. An essential component of this procedure entails adjusting the size of the photos to optimize their proportions, guaranteeing the preservation of their spatial properties. In addition, grayscale feature enhancement techniques are used, which involve the subtle tweaking of several parameters. These methods are conducted with great attention to detail to ensure that image characteristics are reproduced with maximum clarity and distinctiveness, establishing a solid basis for precise and thorough analysis. By employing these strategies to improve the quality of the images, the resulting data becomes more suitable for various uses, such as diagnostic assessments and research projects, thereby adding to the general progress of neuroimaging investigations. Image enhancement encompasses a range of techniques employed to improve the clarity, contrast, brightness, and other relevant attributes of digital images, intending to enhance their visual quality and interpretability.

3.3 Analysis of Pre-trained Models

This work utilized standard transfer learning models, specifically VGG16, VGG19, DenseNet201, ResNet50, ResNet18, Inception V3, AlexNet, and GoogleNet, to identify the most efficient model for classifying brain cancers in the provided dataset. Pre-trained deep learning models are utilized to extract characteristics from images, leading to improved performance accuracies in comparison to conventional models. Furthermore, this results in enhanced comprehensibility, comprehension, and processing of the data.

15

3.3.1   VGG16

VGGNet, abbreviation for Visual Geometry Group, is a CNN structure that was pioneered by Karen Simonyan and Andrew Zisserman. The VGG16 model comprises a total of 16 layers. The primary significance of this study was to demonstrate that the depth of the network plays a crucial role in improving the accuracy of recognition or classification in CNNs. The model undergoes training using the ImageNet dataset in order to accurately categorize images of the natural world. We utilized a pretrained model, excluding the final layers, and incorporated our own layers to categorize images of brain tumors. A dropout layer with a dropout rate of 0.5 has been incorporated to mitigate overfitting. We have incorporated a fully connected layer comprising of 4 output neurons, a Softmax layer to transform the output into probability scores, and a classification layer. Figure 3.2 shows the basic architecture of VGG16 model. The initial LR used is 0.001, a BS of 32, and an Adam optimizer is used. We achieved an accuracy of 92.91% for VGG16 [41].
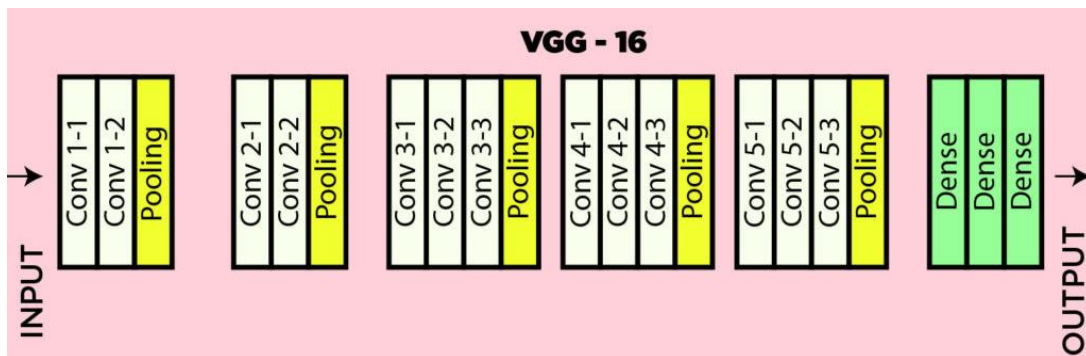
Figure 3.2: VGG16 Architecture

A confusion matrix in deep learning is a tabular representation that evaluates the effectiveness of a classification model. The comparison involves evaluating the predicted and actual class labels, including True Positive, True Negative, False Positive, and False Negative. The matrix enables the computation of measures like accuracy, precision, recall, and F1 score, offering a comprehensive evaluation of the model's capacity to distinguish between different classes. Figure 3.3 and Figure 3.4 shows the CM and the CR of the VGG16 model.

Confusion Matrix

	glioma	meningioma	notumor	pituitary		
glioma	260	35		5	86.7%	13.3%
meningioma	23	266	7	10	86.9%	13.1%
notumor		2	403		99.5%	0.5%
pituitary	4	6	1	289	96.3%	3.7%
	90.6%	86.1%	98.1%	95.1%		
	9.4%	13.9%	1.9%	4.9%		
	glioma	meningioma	notumor	pituitary		

True Class / Predicted Class

Figure 3.3: VGG16 Confusion Matrix

VGG16

	1	2	3	4	5
1	Class	Precision	Recall	F1 Score	Support
2	Glioma	0.9059	0.8667	0.8859	300
3	Meningioma	0.8608	0.8693	0.8650	306
4	NoTumor	0.9805	0.9951	0.9877	405
5	Pituitary	0.9507	0.9633	0.9570	300
6	Overall	0.9245	0.9236	0.9239	1311

Figure 3.4: VGG16 Classification Report

3.3.2   VGG19

The VGG19 model, which is a modified version of the VGG model, is composed of a total of 19 layers. The VGG19 model is composed of a total of 19 layers, including three fully connected (FC) layers at the end. The number of neurons in each of these layers is 4096, 4096, and 1000, respectively. In addition, the model incorporates five MaxPool layers and a Softmax layer. Figure 3.5 shows the basic architecture of VGG19 model [43]. Figure 3.6 and Figure 3.7 shows the CM and the CR of the VGG19 model. VGG19 achieved an accuracy of 90.23%.
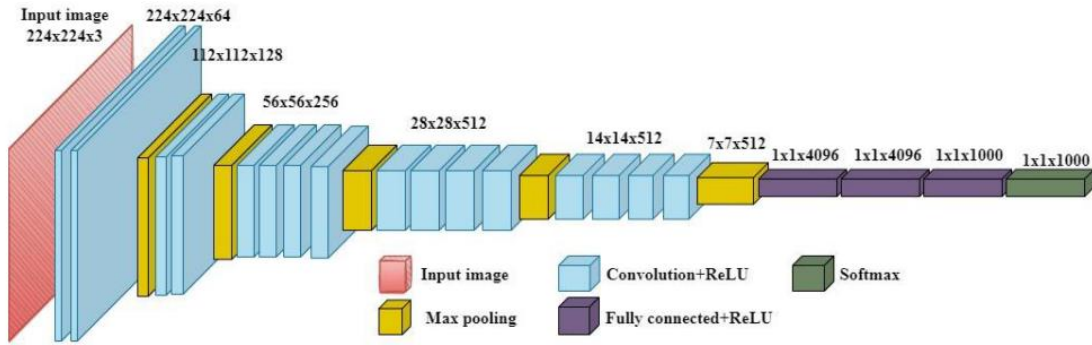
Figure 3.5: VGG19 Architecture

Figure 3.6: VGG19 Confusion Matrix

VGG19

	1	2	3	4	5
1	Class	Precision	Recall	F1 Score	Support
2	Glioma	0.9960	0.8333	0.9074	300
3	Meningioma	0.7092	1	0.8299	300
4	NoTumor	0.9916	0.8875	0.9367	400
5	Pituitary	1	0.8933	0.9437	300
6	Overall	0.9242	0.9035	0.9044	1300

Figure 3.7: VGG19 Classification Report

18

3.3.3   DenseNet201

Densenet201 is a deep transfer learning classifier with 201 layers. DenseNet employs dense connections between layers by means of dense blocks. DenseNet establishes dense connections between each layer and all other layers. This is exceptionally potent. In DenseNet, the input to a layer is formed by concatenating the feature maps from the preceding layers. Through this form of connectivity, DenseNet necessitates fewer parameters compared to a comparable conventional CNN, as it eliminates the necessity of learning redundant feature maps. We utilized a pre-existing model by removing the final levels and incorporating our own layers to categorize brain tumor photos [41]. A dropout layer with a dropout rate of 0.5 has been incorporated to mitigate overfitting. We have added a fully connected layer with 4 output neurons, a Softmax layer to convert the output into probability scores and a classification layer. Figure 3.8 shows the basic architecture of DenseNet201 model. The LR used is 0.001, a BS of 32 and an Adam optimizer is used. We achieved an accuracy of 92.45%.
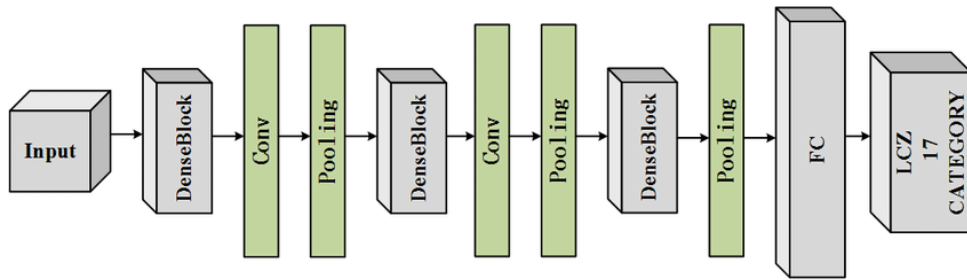
Figure 3.8: DenseNet201 Architecture
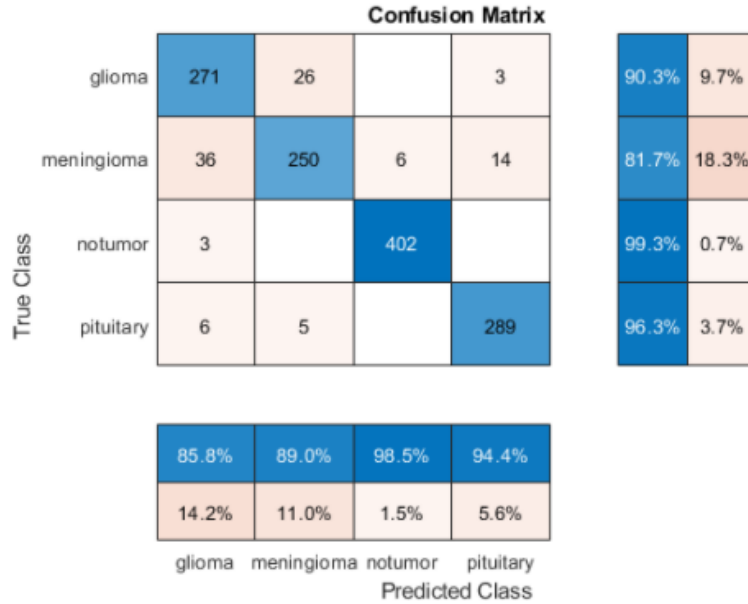
Figure 3.9: DenseNet201 Confusion Matrix

	1	2	3	4	5
	Class	Precision	Recall	F1 Score	Support
1	Glioma	0.8576	0.9033	0.8799	300
2	Meningioma	0.8897	0.8170	0.8518	306
3	NoTumor	0.9853	0.9926	0.9889	405
4	Pituitary	0.9444	0.9633	0.9538	300
5	Overall	0.9193	0.9191	0.9186	1311

Figure 3.10: DenseNet201 Classification Report

3.3.4 ResNet

Resnet50 and Resnet18 are deep neural networks consisting of 50 and 18 layers, respectively. These networks employ shortcut connections to bypass specific layers, reducing the complexity of the network and enabling faster learning. ResNet is an innovative neural network that successfully addresses the problem of "vanishing gradient", enabling the training of numerous layers, ranging from hundreds to thousands. The main feature of this technology is its utilization of residual learning, which allows for more efficient integration of the inputs from previous layers into the network [42]. Nevertheless, a disadvantage of this approach is the substantial computing expense

required for evaluation, which is a result of the large number of parameters involved. We have achieved an accuracy of 91.99 for ResNet18 and 93.14 for ResNet50. Figure 3.12 and Figure 3.13 shows the CM and the CR or the ResNet 50 model.

Figure 3.11: ResNet50 Architecture

Figure 3.12: ResNet50 Confusion Matrix

		1	2	3	4	5
1	Class	Precision	Recall	F1 Score	Support	
2	Glioma	0.9331	0.8367	0.8822	300	
3	Meningioma	0.8424	0.9085	0.8742	306	
4	NoTumor	0.9830	1	0.9914	405	
5	Pituitary	0.9567	0.9567	0.9567	300	
6	Overall	0.9288	0.9255	0.9261	1311	

Figure 3.13: ResNet50 Classification Report

3.3.5   Inception V3

The Inception v3 model is widely recognized for its ability to accurately identify images, with a remarkable accuracy rate of 78.1% on the ImageNet dataset. The model is a convolutional neural network that underwent training using a dataset consisting of more than one million photos sourced from the ImageNet database. The network possesses a depth of 48 layers and exhibits the ability to classify pictures into 1000 discrete object categories, encompassing, but not restricted to, keyboard, mouse, pencil, and diverse animals. As a result, the network has obtained extensive and complex feature representations for a wide range of images. The dimensions of the network's picture input are 299 by 299. Figure 3.14 depicts the fundamental structure of the Inception v3 model. The model consists of both symmetric and asymmetric elements, including convolutions, average pooling, max pooling, dropouts, and fully connected layers. The utilization of BN is widespread in the model, where it is applied to the inputs of the activation functions. The calculation of loss is performed using the Softmax function.
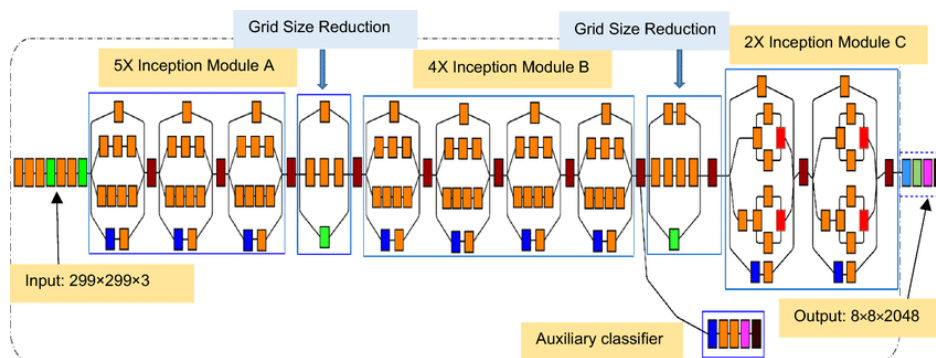
Figure 3.14: Inception V3 Architecture

We have achieved an MRI brain tumor classification accuracy of 92.60%. Figure 3.15 and Figure 3.16 shows the CM and the CR of the Inception v3 model.

Figure 3.15: Inception V3 Confusion Matrix

Figure 3.16: Inception V3 Classification Report

3.3.6   GoogleNet

In 2015, Google unveiled GoogleNet, a deep neural network comprising 22 layers. This convolutional neural network exhibits a unique architecture that incorporates parallelization. The model prominently includes an inception block that combines convolution filters with dimensions of 1×1, 3×3, and 5×5, together with a max-pooling layer of size 3×3. This design innovation enhances the network's performance in picture recognition tasks by enabling it to capture information across various scales and complexities [41]. After applying GoogleNet of the given dataset and accuracy of 91.46% was achieved. Figure 3.17 and Figure 3.18 shows the CM and the CR of the GoogleNet model.

Figure 3.17: GoogleNet Confusion Matrix

Figure 3.18: GoogleNet Classification Report

3.3.7   AlexNet

AlexNet, developed by Alex Krizhevsky, Ilya Sutskever, and Geoff Hinton, is largely acknowledged as the pioneering convolutional neural network that gained substantial recognition in the domain of computer vision. There are a total of nine layers in the architecture, including five convolutional layers, three pooling layers, and three fully linked layers. AlexNet, unlike LeNet, is considerably larger and deeper, representing a notable progress in the capability and depth of neural networks for image identification applications. After applying AlexNet of the given dataset and accuracy of 92.60% was achieved. Figure 3.19 and Figure 3.20 shows the CM and the CR of the GoogleNet model.
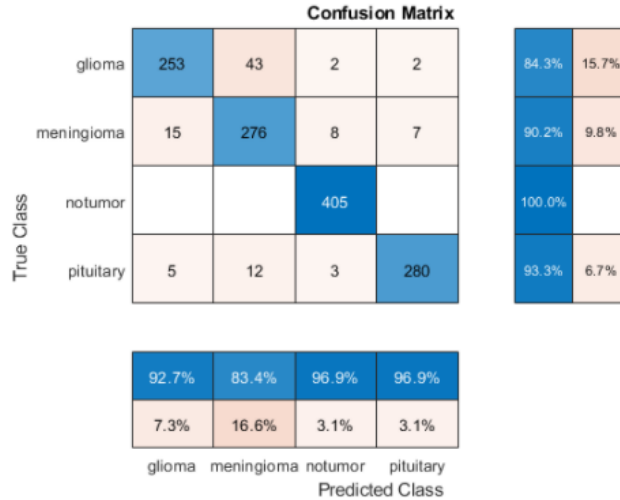
Figure 3.19: AlexNet Confusion Matrix

Figure 3.20: AlexNet Classification Report

Table 3.4: Comparative Analysis of Transfer Learning Models Batch Size 16

Models	Batch Size	Accuracy
VGG16	16	86.42%
VGG19	16	91.91%
DenseNet201	16	90.39%
ResNet50	16	93.14%
ResNet18	16	91.99%
Inception V3	16	92.14%
GoogleNet	16	91.46%
AlexNet	16	92.60%

Table 3.5: Comparative Analysis of Transfer Learning Models Batch Size 32

Models	Batch Size	Accuracy
VGG16	32	92.91%
VGG19	32	92.45%
DenseNet201	32	92.45%
ResNet50	32	92.30%
ResNet18	32	92.60%
Inception V3	32	92.60%
GoogleNet	32	93.29%
AlexNet	32	92.60%

Although these models have shown remarkable accuracy in image categorization, they have limitations in their capacity to identify and precisely locate certain features inside images. For brain tumor MRI scans, these models do not have the ability to offer bounding box predictions and accurate tumor localization. In order to overcome this constraint, there is an urgent want for sophisticated models that possess the capability to not only categorize but also precisely identify, pinpoint, and ascertain the dimensions of brain tumors in MRI images. Integrating bounding box prediction skills into models can greatly improve their usefulness in medical imaging, allowing for more extensive diagnostic applications.

Chapter 4

Brain Tumor Detection and Classification Using YOLOv7

4. YOLO

YOLO was proposed as a novel method for object detection in 2015. YOLO stands for You Only Look Once. It performs cohesive, and real-time Object Detection. YOLO acquires class probability and boundary box directly from pixels of the image, rather than using a combination of classification and proposal, which differs from R-CNN. As input, YOLO accepts a full image. It predicts various bounding boxes using a single convolutional network. It also predicts their class probabilities. This approach provides YOLO with a number of benefits. For starters, it reduces the process of detection to a regression problem, eliminating the need for complex pipelines. Second, YOLO can include global information about the entire image to make predictions. This process reduces the errors in the background. Furthermore, YOLO chooses GoogLeNet as its base network rather than VGG-16 because the former is much faster. So, YOLO is designed to be fast and real-time while maintaining high accuracy. YOLO has a higher chance of generating localization errors than other techniques based on region proposals. The YOLO loss function treats large and small bounding box errors equitably, resulting in a positioning that is not accurate. YOLO might ignore some objects in detection, i.e. when there are numerous objects in just one grid cell, detection recall decreases. This disadvantage is difficult to avoid because YOLO assumes that all bounding boxes that belong to the same cell are from the same class [13]. To accomplish the purpose of object detection, YOLO employs three main terminologies. To understand how this model performs with high accuracy and at a faster rate, in comparison to other algorithms, it is crucial to understand these three techniques. The first concept is residual blocks. 7×7 residual blocks are used in the first architectural design to generate the grids in the specific image. Each grid functions as a central point of focus. Each of these grids is assigned a specific forecast. The second strategy involves generating bounding boxes by taking into account each focal point associated with a particular forecast. While classification tasks are generally effective across all grids, the process

of dividing the bounding boxes for each prediction poses greater challenges. The third and final method involves utilizing IoU to identify the bounding boxes that are optimal for the given detection task. When compared to other approaches for training and algorithms for object detection, YOLO's speed of processing and computation is quite fast, especially in real time. Aside from its computing speed, the YOLO method also provides overall high accuracy by reducing background errors. The architecture of this model enables it to gain insight and understand multiple objects more effectively.
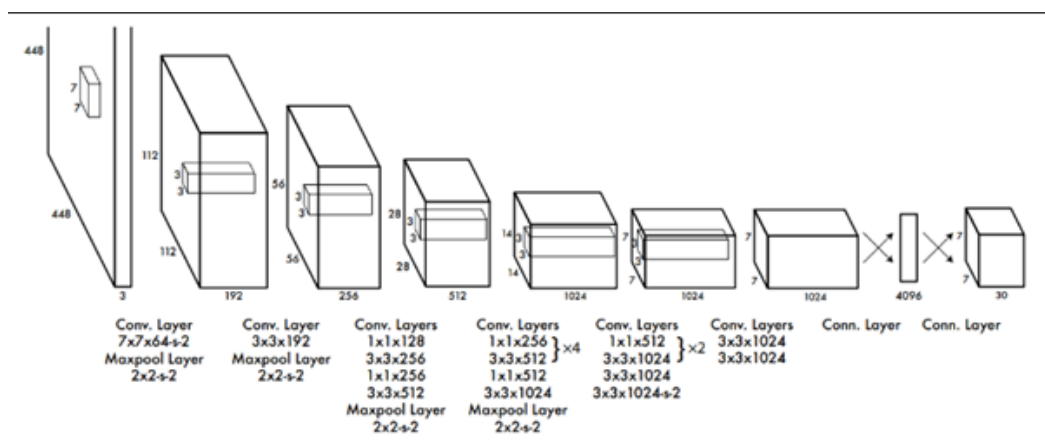
Figure 4.1: YOLO System Model

4.1 Why YOLO

DL based object detection surpasses standard ML techniques in terms of both accuracy and speed. DL is a neural network based on forward feedback and it is the latest and widely used method. It has a distinct advantage in the recognition of objects due to its unique structure of local weight sharing. CNN consists of a pooling layer, a convolution layer, and an FC layer. Present object detection algorithms rely on CNN. Object detection is split into two parts: location and classification. Conventional detectors collect features and proposals first and then classify them. It is prone to errors and slow. Some algorithms of object detection that are based on region, like Fast-RCNN, accomplish CNN classification while collecting the proposals via the selective search method. It takes a long time to extract proposals. YOLO proposed to combine classification and location in a single CNN. That's why YOLO is very fast. While all of the object detection methods proposed previously perform satisfactorily on images as well as video analysis, however, to perform spontaneous object detection, the YOLO is the most preferred technique. It reaches high accuracy for most of the tasks that are processed in real time and keeps its fps and speed reasonable

depending on the device. This model is unified and has numerous benefits over conventional methods of object detection and these are the main reasons I used YOLO for my task. First, it is incredibly quick. We do not require an intricate pipeline if we conceptualize detection to be a regression problem. To forecast detections, the neural network must be utilized on a novel image during the testing phase. When using a Titan X GPU, the base network achieves a frame rate of 45 frames per second without any batch processing. However, for a faster version, the frame rate exceeds 150 frames per second. Consequently, it is feasible to perform real-time processing of the streaming video while maintaining a latency of no more than 25 ms. Moreover, YOLO outperforms other systems of spontaneous object detection by more than twice their mAP. Second, YOLO considers the image as a whole while making predictions. Dissimilar to the techniques that also use the sliding window and the methods that use the region proposal, YOLO is able to encode the look and contextual information of classes since it processes the full image during training and testing. Because it cannot reach the broader context, Fast R-CNN, although it is a top method of object detection, confuses the background regions in the image with objects. YOLO exhibits a reduction of around 50% in background errors when compared to Fast R-CNN. Furthermore, YOLO acquires knowledge of universal object representations. The YOLO model outperforms leading detection approaches such as DPM and R-CNN when trained on real photos and tested on artwork. This model has less chance of failure when employed on new domains or unanticipated data because it is extremely universal. Due to these benefits, the structure of YOLO has emerged as one of the most successful and powerful algorithms for object detection.

4.2   YOLOv7 Model

YOLOv7 architecture consists of a powerful backbone designed to capture hierarchical features from input images. Multiple convolutional layers with progressively larger receptive fields are included in the backbone, which enables the model to identify both coarse-grained and global information. Batch normalization layers are positioned carefully to speed up and stabilize the training process. Anchor boxes are used by YOLOv7 to forecast bounding box coordinates and related class probabilities. During the training phase, the anchor boxes are carefully selected to correspond with the dataset's predicted item sizes. Multiple convolutional layers make up the detection head, which is in charge of enhancing bounding box coordinates and forecasting class probabilities. YOLOv7 integrates a Feature Pyramid Network (FPN) to address scale changes in sizes within medical images. By merging information from several backbone levels, FPN improves

the model's capacity to identify tumors of various sizes. This is especially important for precisely identifying tiny tumors or ones that are spread throughout the brain. The YOLOv7 model integrates various strategies, including E-ELAN [23], model scaling by concatenation [24], and model re-parameterization [25], to achieve a trade-off between detection efficiency and precision. Figure 4.2 illustrates the YOLOv7 network, which is made up of four distinct modules—the input, head, backbone, and the prediction—is shown in Figure 4.2.
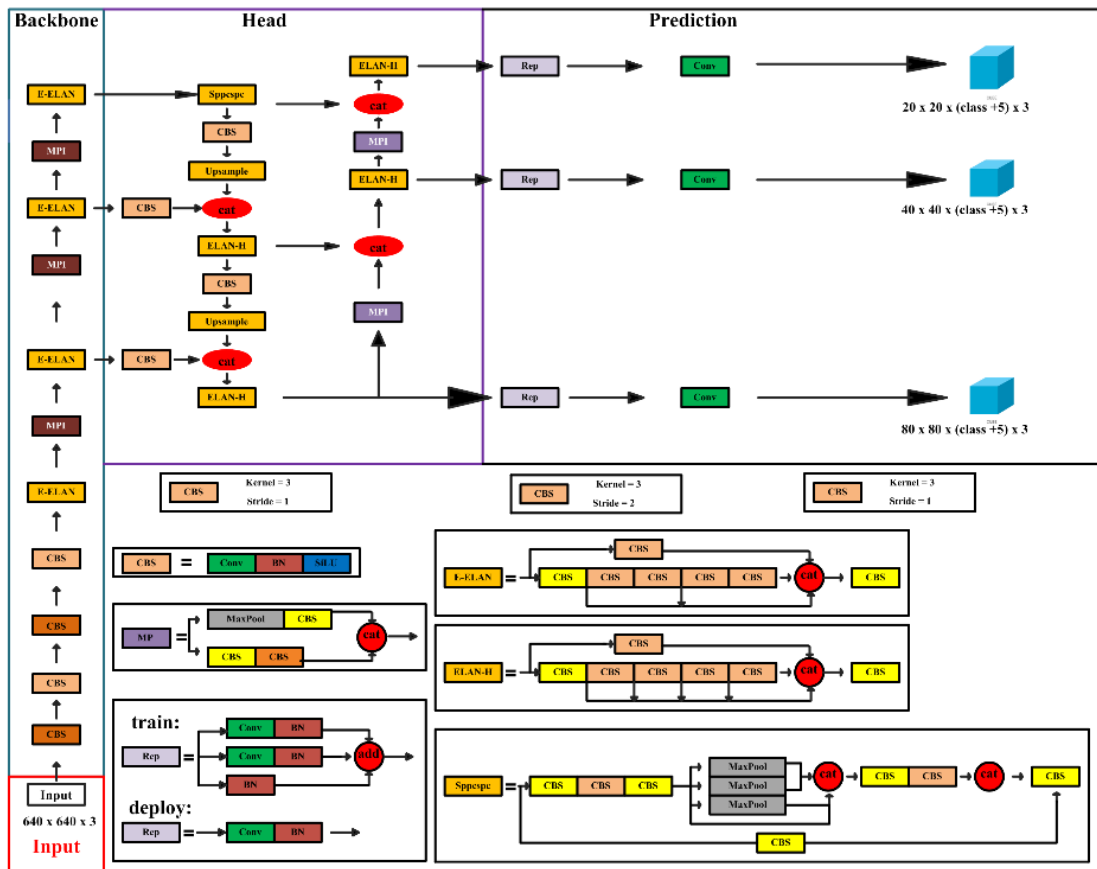
Figure 4.2: Network Architecture of YOLOv7

Input: The YOLOv7 model augments data in the very first processing stage using mosaic and hybrid methods. To further guarantee that all input color images are uniformly resized to 640x640 dimensions, it employs the adaptive anchor box mechanism, first introduced by YOLOv5.This assures that the input size of the backbone network satisfies the specified criteria.

Backbone: The YOLOv7 network consists of three primary parts. MP1, E-ELAN, CBS, and CBS. Activation functions, batch normalization, and convolution make up the CBS module. While improving the network's ability to learn, the E-ELAN module keeps the original ELAN structure.

30

It does this by preserving the original gradient route while instructing different computational blocks of feature groups to learn a wider range of features. There are two divisions within MP1, one for the CBS division and one for the MaxPool division. The upper branch uses MaxPool to cut the image in half along the length and width axes. In addition, the image channels are cut in half using CBS, which has 128 output channels. Using a 1x1 kernel and stride, the lower branch halves the image channels. After that, it uses a 3x3 kernel and a 2x2 stride to halve the image dimensions. Ultimately, it merges the extracted characteristics from both branches by employing the Cat operation. MaxPool performs max-pooling, which selects the highest value within tiny local areas. On the other hand, CBS performs complete bilinear sampling, which captures all the valuable information within small local areas. This improves the network's capacity to extract features.

Head: The head network of YOLOv7 is constructed by employing the FPN architecture, which integrates the PANet design. This network consists of multiple CBS blocks. The system utilizes a Sppcspc structure, a highly efficient layer aggregation network, & the MaxPool-2. The inclusion of a CSP framework within the SPP framework enhances the network's capacity to perceive information, thereby improving its overall effectiveness. Furthermore, it incorporates a substantial remaining boundary to assist in the process of optimization and the extraction of features. The ELAN-H layer is formed by aggregating multiple feature layers derived from E-ELAN, resulting in improved feature extraction. The MP2 block shares a comparable structure with the MP1 block, albeit with a minor alteration in the quantity of output channels [26].

Prediction: The prediction network of YOLOv7 makes use of a Rep architecture for adjusting the number of image channels for the features generated by the head network. Subsequently, a 1x1 convolution is employed to predict the levels of confidence, category, and anchor frame. The Rep structure, which draws inspiration from RepVGG [27], contains a unique residual architecture for the enhancement of the training process. The specific residual architecture can be simplified to a basic convolution in actual forecasts, leading to a reduction in network complexity without sacrificing predictive efficiency.

The Mish activation function, which YOLOv7 introduces, has been found to perform better in terms of convergence and model performance than more conventional activation functions like ReLU. By applying the Mish function on the intermediate feature maps, feature maps, the model's non-linearity is improved and improved feature representation is encouraged.

4.3   Model Training

Pre-trained weights from extensive object identification datasets, such as MS COCO, are used to initialize the YOLOv7 model. By allowing the model to inherit information about general object properties, this transfer learning technique speeds up convergence and enhances the model's tumor detection capabilities. The system model for the suggested MRI brain tumor detection based on YOLOv7 is illustrated in Figure 4.3. The diagram visually depicts the proposed system model. An adaptive learning rate technique is utilized to maintain stability during the training period. The learning rate is gradually increased during the warm-up phase to allow the model to explore the loss landscape more effectively. In the course of succeeding epochs, training starts with lower picture resolutions and gradually raises them. The model performs better on a variety of brain scans because of this incremental scaling strategy, which also improves the model's generalization across scales.
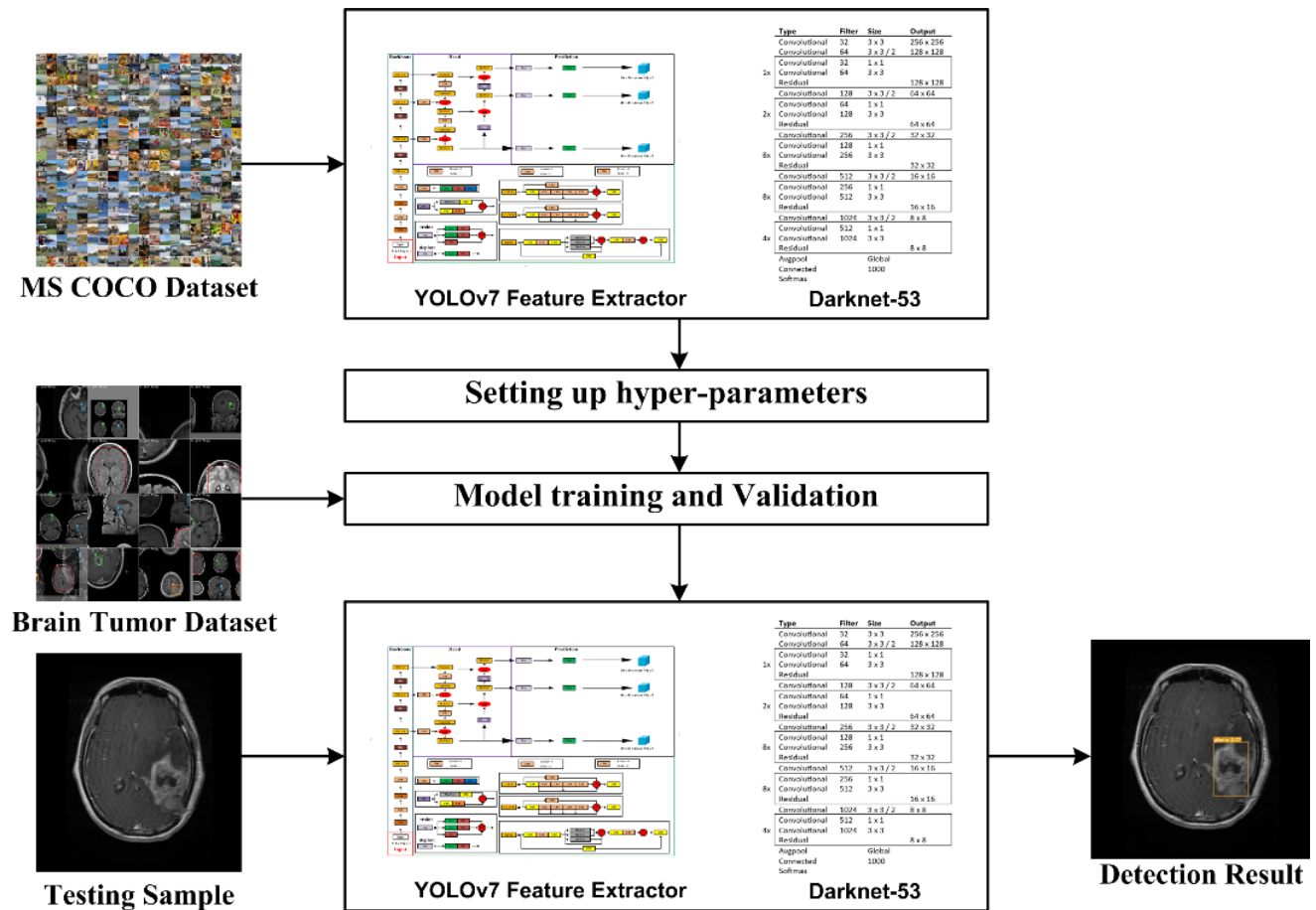

Figure 4.3: System Model of MRI Brain Tumor Detection Using Yolov7

32

4.3.1   Feature Extractor: Darknet53

The Darknet-53 network is a crucial component of the YOLOv7 object detection system, serving as the primary feature extractor. It is responsible for extracting hierarchical characteristics from input images. Darknet-53, as shown in Figure 4.4 is a neural network structure consisting of 53 convolutional layers, is highly proficient in capturing complex features that are crucial for object detection. After every convolutional layer, batch normalization, and activation layer comes. It has 3x3 and 1x1 filters. The stack of convolutional layers in the backbone network is purposefully crafted to acquire and extract characteristics from input images, utilizing convolutional operations that apply filters, or kernels, across the input image to identify patterns. Darknet-53, which draws inspiration from the ResNet architecture, features residual connections. These connections allow the network to bypass certain layers during training, effectively tackling issues such as the vanishing gradient problem. The architecture is strategically designed to capture features at various spatial scales, essential for identifying objects of varying sizes in an input image. By integrating down-sampling layers like max-pooling or convolutional strides, darknet-53 effectively decreases the spatial dimensions of feature maps. This enables the extraction of features at various resolutions. The darknet-53 model is renowned for being capable of extracting a diverse range of key features from the images. It acts as the foundation for subsequent stages in the YOLOv7 architecture, allowing accurate predictions regarding object classes and bounding box coordinates in real-time object detection scenarios.

	Type	Filter	Size	Output
	Convolutional	32	3 x 3	256 x 256
	Convolutional	64	3 x 3 / 2	128 x 128
1x	Convolutional	32	1 x 1	
	Convolutional	64	3 x 3	
	Residual			128 x 128
	Convolutional	128	3 x 3 / 2	64 x 64
2x	Convolutional	64	1 x 1	
	Convolutional	128	3 x 3	
	Residual			64 x 64
	Convolutional	256	3 x 3 / 2	32 x 32
8x	Convolutional	128	1 x 1	
	Convolutional	256	3 x 3	
	Residual			32 x 32
	Convolutional	512	3 x 3 / 2	16 x 16
8x	Convolutional	256	1 x 1	
	Convolutional	512	3 x 3	
	Residual			16 x 16
	Convolutional	1024	3 x 3 / 2	8 x 8
4x	Convolutional	512	1 x 1	
	Convolutional	1024	3 x 3	
	Residual			8 x 8
	Avgpool		Global	
	Connected		1000	
	Softmax			

Figure 4.4: Darknet-53 Architecture

33

4.3.2 Detection Approach

This section gives a brief overview of the detection mechanism utilized by the YOLO model. The approach begins by having the model analyze a picture using logical SxS grids and weighted feature sets to determine the likelihood within specific cells. When the centroid of a prospective entity aligns with one of these cells, the model generates an initial bounding box that encompasses the prediction probability derived from its training.

$$S \times S \times \left(K \times (4 + 1 + N)\right) \qquad 4.1$$

Afterward, the model utilizes different scaled boxes to generate predictions and obtain a $3D$ tensor using equation (1), it utilizes the variable N to indicate the number of classes. Within this equation, four variables t_x, t_y, t_w, t_h are used to denote the prediction coordinates of the detecting boxes. Additionally, there is one variable that represents the confidence of the prediction for each bounding box [9]. The bounding box prediction shown in Figure 4.5 obtained from the width pw and height ph. It also incorporate offsets cx and cy which are measured relative to the cluster center. In instances when the cell is offset from the top left by (c_x , c_y) and the detection bounding box is characterized by the values pw and ph, the prediction is determined by the formulation outlined in equation (2) [10].

$$b_x = \sigma(t_x) + c_x$$
$$b_y = \sigma(t_y) + c_y \qquad 4.2$$
$$b_w = P_w e^{tw}$$
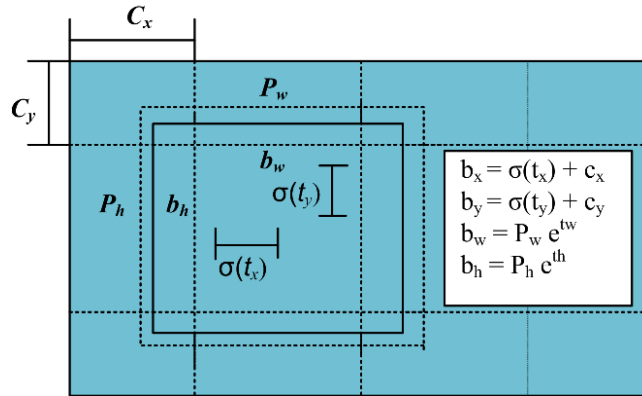$$b_h = P_h e^{th}$$

Figure 4.5: Bounding box prediction

Concurrently, as stated in equation (3), the IoU is used to measure the degree to which the prediction aligns with a ground truth image from the dataset during the creation of bounding boxes.

$$IoU_{Pred}^{truth} = \frac{area(B^{truth} \cap B^{pred})}{area(B^{truth} \cup B^{pred})} \qquad 4.3$$

The value of C in each grid cell is determined by $P_r(Class_i|Object)$. Only predictions that are greater than a predetermined threshold will result in an initial bounding box, even if there are several predictions for a certain object. The condition is properly expressed by equation (4).

$$P_r(Class_i|Object) \times IoU_{pred}^{truth} = P_r(Class_i) \times IoU_{pred}^{truth} \quad 4.4$$

During the initial detection phase, there are often numerous probable object predictions that may occur. Although, by implementing the non-maximum suppression technique, the detection model efficiently chooses the prediction with the highest confidence score, thereby eliminating unnecessary boxes.

The analytical process is executed within the Google Colab environment, leveraging the additional capabilities of GPUs to enhance overall performance speed. PyTorch is a deep learning framework that is used for training and assessment. Version control systems are used to monitor modifications to the model architecture and hyperparameters, and custom scripts and utilities are created to make the experimenting process easier. Within our novel methodology, we employ transfer learning as an initial step to train the model, ensuring its accuracy in subsequent testing phases.

4.4   Evaluation Metrics

Upon the completion of the training and testing stages, the subsequent stage involves conducting a thorough performance assessment using standardized evaluation metrics tailored for object detection. This evaluation aims to gauge the complete effectiveness of the model. The metrics employed for performance evaluation encompass IoU, mAP, precision, recall, and F1-measure. The ratio of the overlapping area between the trained annotated data and predicted bounding boxes to the entire area covered by both is used to compute the area of overlap or IoU. Mean Average Precision is employed to evaluate the overall precision-recall performance across different classes. The metrics are computed based on the count of TP, FP, and FN predictions made by the model on testing data. TP represents accurately detected tumor instances with correct labels, while FP includes instances of falsely detected MRI scans, and FN accounts for images that the model failed

to detect. The F1-score is a key measure for evaluating the harmonic mean between FN and FP in an imbalanced dataset, as compared to accuracy [11]. Meanwhile, the mAP calculates the average of all APs for each category. Employing mAP as the main indicator helps validate a model's effectiveness in overall brain tumor detection. Equation (5) formally expresses the mathematical formula for mAP.

$$mAP = \frac{1}{N} \sum_{i=1}^{N} APi \qquad 4.5$$

In the medical area, metrics like precision, recall, and F1-measure are important for evaluating the accuracy of positive predictions relative to all detections, potential detections, and the trade-off between precision and recall, respectively. Similarly, within the realm of Deep Learning (DL), these metrics contribute to gauging the effectiveness of a model and establishing its reliability for a specific task. The formal calculations are based on equations (6), (7), and (8) [12]. Recall assesses the ability to identify all positive results, precision measures the accuracy of predictions, and the F1 measure, which is calculated as a harmonic mean of P and RC, provides a well-balanced assessment of both traits.

$$PR = \frac{TP}{TP + FP} \qquad 4.6$$

$$RC = \frac{TP}{TP + FN} \qquad 4.7$$

$$F1 - measure = \frac{2 \times PR \times RC}{PR + RC} \qquad 4.8$$

Chapter 5

Results and Discussion

5. Results

This section presents an in-depth overview of the results gathered from the research conducted. To assess the adequacy of the model's training with the provided data, graphical representations of loss convergence were utilized. As illustrated in Figure 5.1, the blue line in the graph suggests minimal loss or errors during the validation of the image dataset. This characteristic loss pattern is considered optimal, indicating accurate and precise validation of images with minimal errors, portraying a gradual learning process without encountering fitting issues. Concurrently, the red line denotes a gradual increase in model precision over time from the training dataset. Figure 5.1 demonstrates the lowest average loss of 0.0993. The outcome affirms the effective training of the model, successful utilization of the CIoU loss function [13], absence of overfitting or underfitting indications, and a quick convergence during the training phase.
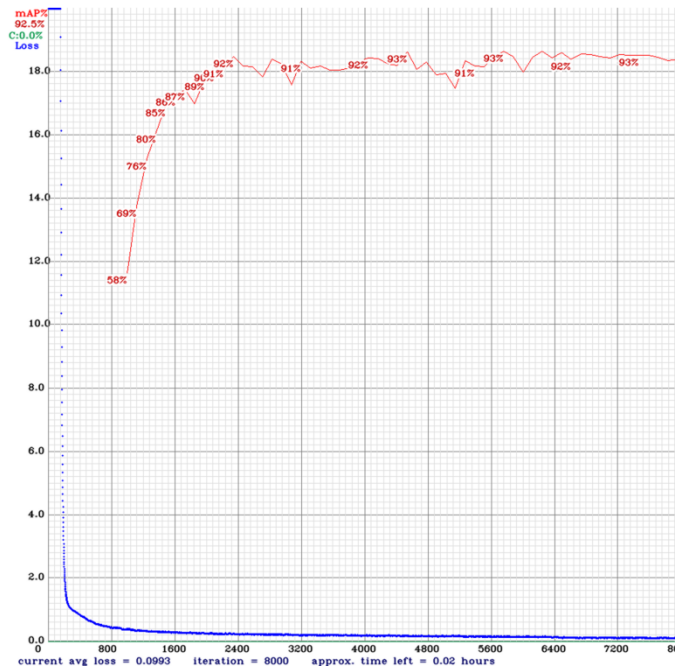

Figure 5.1: Loss precision graph

Following the successful completion of the training, we continued to assess the efficacy of the training procedure. We employed the Python utils library to provide visual representations of the validation metrics. As the number of epochs increases the box loss and class loss decrease in both training and validation, and the precision and recall increases which eventually increase the accuracy of the model. The validation metrics are presented in Figure 5.2.
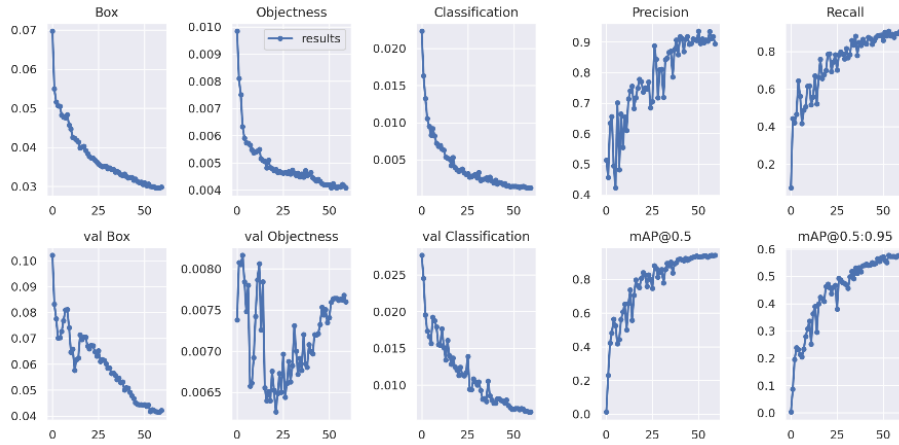

Figure 5.2: Evaluation matrices of YOLO

To enhance the clarity of our findings, we utilized various metrics such as P, RC, mAP, F1 measure, and a confusion matrix.
Figure 5.3 depicts the ratios of TP and TN values, as well as FP and FN values for the various types of brain tumors namely pituitary, meningioma, glioma respectively. The confusion matrix demonstrates the model's outstanding performance, demonstrating its accurate identification of different brain tumor MRI scans with exceptional precision.
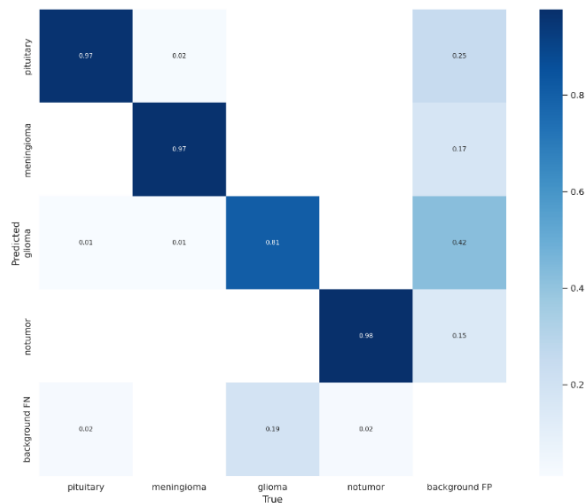

Figure 5.3: Confusion Matrix

Figure 5.4 and Figure 5.5 depicts the Precision and Recall confidence curves. Precision is a metric that quantifies the model's ability to accurately predicts a specific class among all the correct predictions made. A high level of precision demonstrates the model's ability to accurately forecast classes that correspond to the true classes.
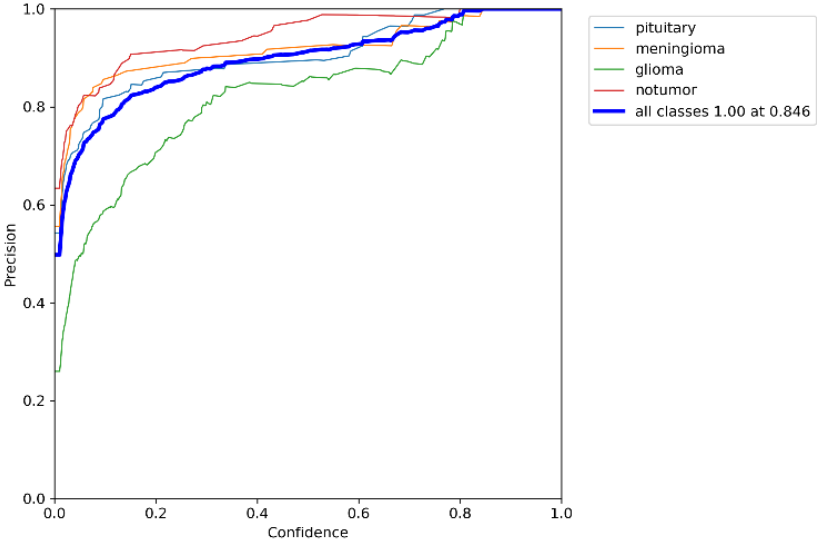

Figure 5.4: Precision Curve

Recall is a quantitative measure that indicates the number of correct predictions among all the predictions made. A higher recall indicates that a significant proportion of the predictions accurately match the true class.
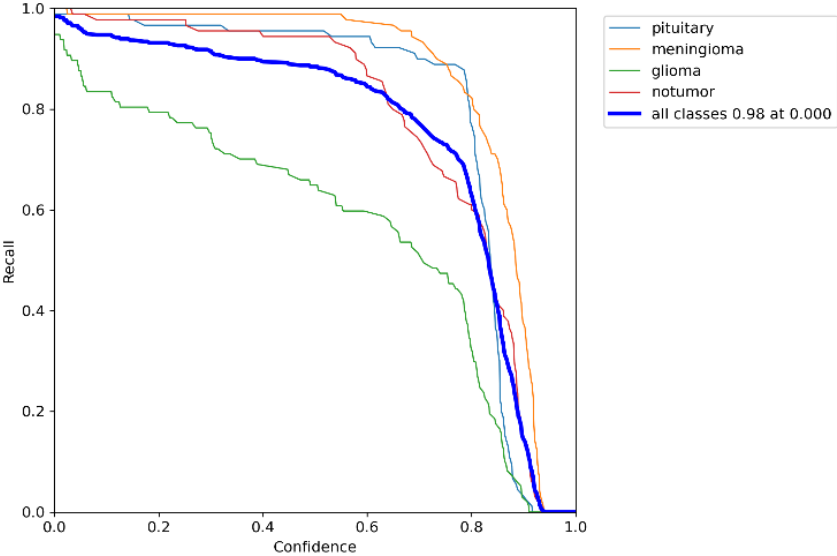

Figure 5.5: Recall Curve

The F1 confidence curve and the mAP of the proposed model are illustrated in Figure 5.6 and Figure 5.7. The model's F1 score is notably impressive, standing at 90%. The F1 measure helps determine the ideal threshold that achieves high precision and adequate recall simultaneously. The F1 measure provides a balanced assessment of P and RC by using the harmonic mean, making it a critical measure for assessing the effectiveness of an object identification model.
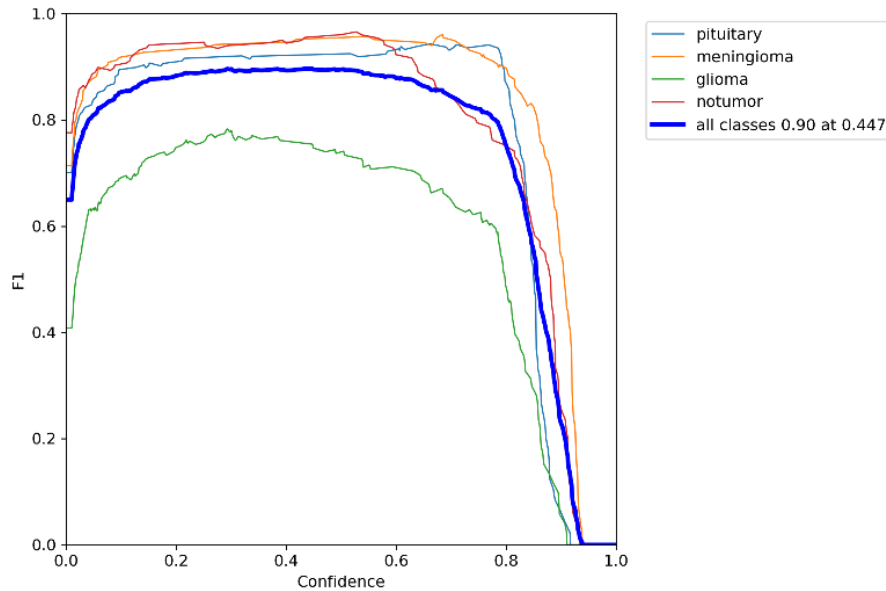
Figure 5.6: F1 Score Curve

The mAP is computed using the PR curve, a frequently used evaluation metric for the identification and multi-class classifications. The evaluation method calculates the average precision at different recall levels to determine the model's accuracy. This provides a thorough assessment of the model's performance for all the classes. A larger proportion of the region under the curve signifies better performance. The suggested approach illustrates a harmonious trade-off between P and RC.

Figure 5.7: Precision-Recall Curve

The YOLOv7 object detection model demonstrated outstanding performance on the test images, with an impressive mAP of 94.30%. Upon evaluating the model on the test dataset, the output images displayed bounding boxes surrounding tumor areas, so indicating the presence of a brain tumor in the MRI scan images. Figure 5.8 pre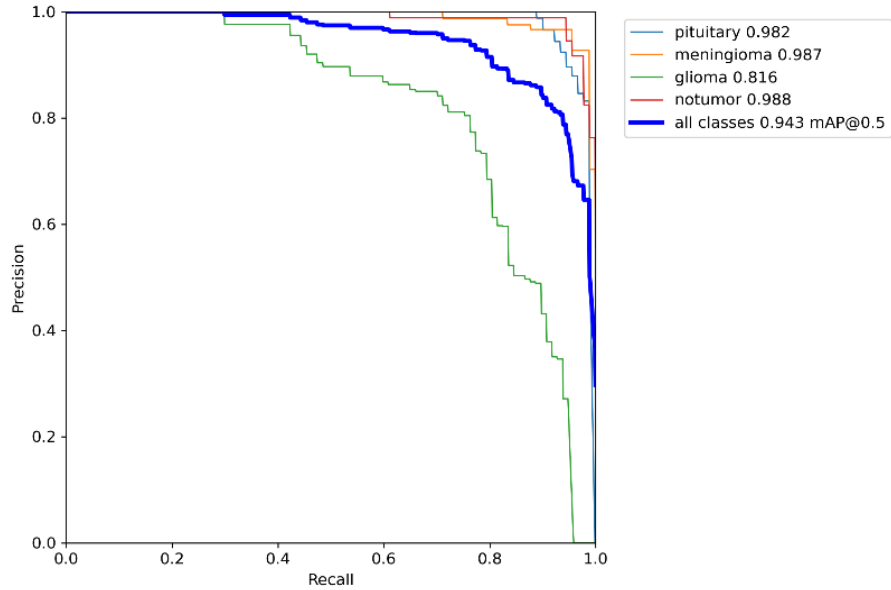sents the ground truth of the images in the training dataset, while Figure 5.9 exhibits the result produced by the model. Significantly, the resulting images displayed bounding boxes together with a confidence score, which offered valuable information on the precision of the identified areas. The model was able to reach a mean average precision of 81.7% for glioma, 98.6% for meningioma, 98.1% for pituitary, and 98.6% for brain with no tumor. The YOLOv7 model achieved impressive overall P, RC, F1 measure, and mAP values, with scores of 90.7, 89.2, 90, and 94.3 respectively. The performance metrics are presented in Table 5.1.
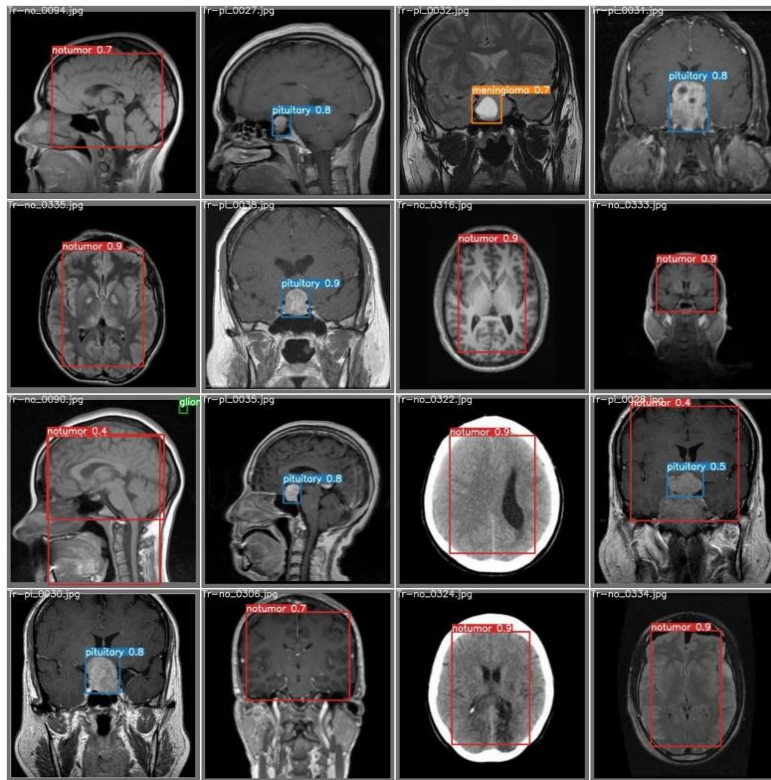
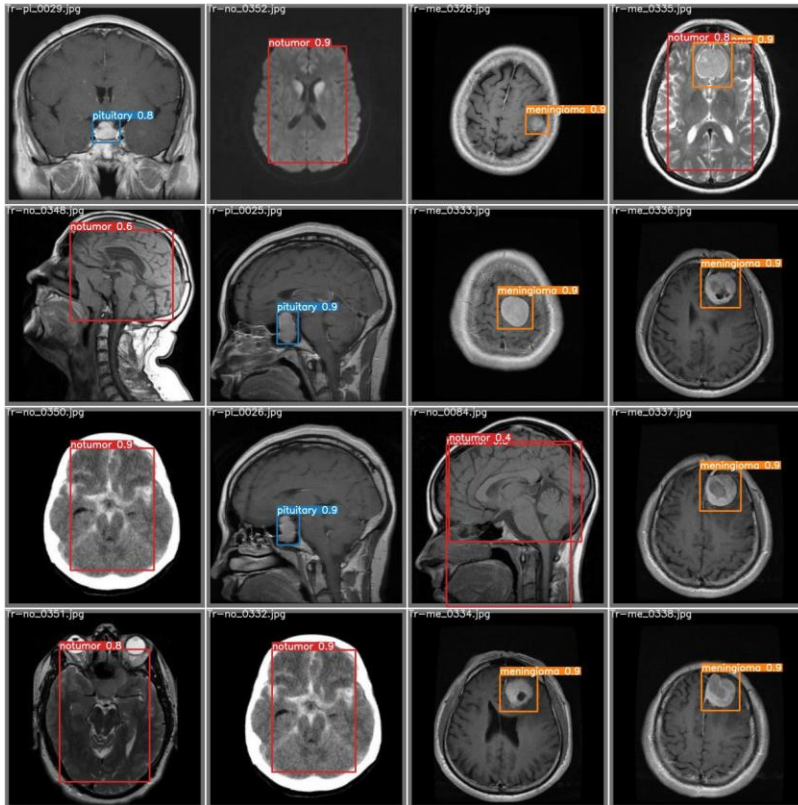*Figure 5.8: Ground Truth Data for Training*

Figure 5.9: Output Generated By the model on Test Data

After that, we tested the model by giving individual images of the brain tumor for the detection purpose and the model performed exceptionally well by detecting the exact true class of brain tumor with a good confidence score. The proposed model detected even a small tumor correctly by making a bounding box with the label and a confidence score. Figure 5.10 shows the detection of each tumor class and a healthy brain with no tumor with the confidence score detected by the proposed model.

Glioma   **Meningioma**   **Pituitary**   **No Tumor**
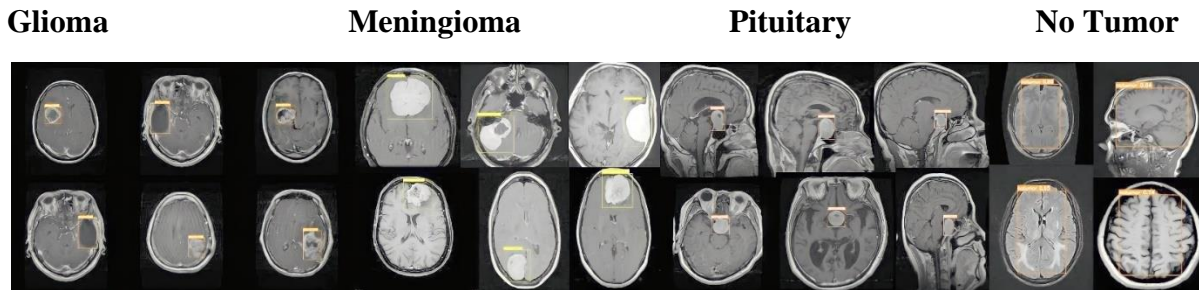
Figure 5.10: Detection from an Individual Tumor Class

Table 5.1: Overall Performance Achieved by Proposed Model

Model	YOLOv7 Object Detector
Precision	90.7
Recall	89.2
F1 Score	90
mAP	94.3

5.1 Performance Comparison with Other Models

This section provides a comprehensive comparison of the results obtained in this study with some existing studies that focused on brain tumor detection from MRIs. It should be noted that making a direct comparison is difficult because of the differences in methodologies used in various studies. The main objective is to demonstrate the improvement in brain tumor detection achieved through object detection in the suggested approach. It is worth mentioning that just a few studies have used bounding boxes for brain tumor detection in MRIs, as the majority of studies usually rely on classification and segmentation techniques. Table 5.2 highlights some of the few studies that have

integrated object detection techniques using bounding boxes to accurately identify the precise location of brain tumors in MRI data. By implementing the YOLOv7 model, this study produced an impressive mAP of 93.14%, surpassing the rates obtained by other studies. The results highlight the remarkable performance of the YOLOv7 model in this study, surpassing existing approaches for detecting brain tumors in MRI images.

Table 5.2: Performance Comparison With existing object detection approaches

Model	Dataset Size	No of Classes	Result
F-R-CNN [14]	3064	3	91.66%
F-R-CNN [15]	2406	3	77.60%
YOLOv5 [16]	1992	2	85.95%
Proposed YOLOv7	7023	4	94.30%

Chapter 6

Conclusion and Future Work

This study demonstrated the effectiveness of employing TL and fine-tuning the YOLOv7 model to accurately detect various types of brain tumors, including glioma, meningioma, and pituitary tumors, in MRI data. The dataset possessed various viewpoints, including axial, coronal, and sagittal, for each tumor type. Various data pre-processing techniques were employed, such as applying min-max normalization to enhance pixel contrast, converting files, and generating training labels for tumor coordinates. The model employed pre-trained weights from MSCOCO using transfer learning, together with newly initialized feature sets derived from the MRI dataset. The YOLOv7 model achieved a 94.30% mean average precision (mAP) at a 0.5 threshold during evaluation by effectively detecting distinct brain tumors. This was made possible through end-to-end optimal training via fine-tuning. The study's results demonstrate that the pre-trained and fine-tuned object detection algorithms, such as YOLOv7, are highly proficient in precisely detecting brain tumors in MRI images. Unlike classification methods, this strategy not only identifies the location of brain tumors but also categorizes them into particular groups, reducing the need for interpretation. In addition, the suggested solution is versatile across several platforms as it has little space needs and cheap computational costs, unlike segmentation methods. Although this work demonstrated superior precision compared to other systems that use bounding box detection for various brain tumors, it does recognize some limits. Utilizing bounding boxes limits the accurate delineation of tumors in comparison to a segmentation methodology. In addition, training YOLO-based models requires careful and detailed dataset labeling, which is more extensive than the labeling process for a classification technique. Despite these compromises, the solution proposed by YOLO can expand and develop through ongoing research to tackle these issues. This technology has the capability to help radiologists and medical experts in optimizing their workflow and enabling early treatment. In future advancements, training the model on images with adversarial attacks could enhance its robustness to noise, allowing it to effectively detect tumors in MRI scans even when faced with distorted or adversarially altered images. This approach aims to strengthen the model against potential real-world challenges, ensuring reliable performance.

Bibliography

[1]   S. Grampurohit, V. Shalavadi, V. R. Dhotargavi, M. Kudari, and S. Jolad, "Brain Tumor Detection Using Deep Learning Models," in *Proceedings - 2020 IEEE India Council International Subsections Conference, INDISCON 2020*, Institute of Electrical and Electronics Engineers Inc., Oct. 2020, pp. 129–134. doi: 10.1109/INDISCON50162.2020.00037.

[2]   A. Saleh, R. Sukaik, and S. S. Abu-Naser, "Brain tumor classification using deep learning," in *Proceedings - 2020 International Conference on Assistive and Rehabilitation Technologies, iCareTech 2020*, Institute of Electrical and Electronics Engineers Inc., Aug. 2020, pp. 131–136. doi: 10.1109/iCareTech49914.2020.00032.

[3]   F. J. P. Montalbo, "A computer-aided diagnosis of brain tumors using a fine-tuned yolo-based model with transfer learning," *KSII Transactions on Internet and Information Systems*, vol. 14, no. 12, pp. 4816–4834, Dec. 2020, doi: 10.3837/tiis.2020.12.011.

[4]   P. Modiya and S. Vahora, "International Journal of INTELLIGENT SYSTEMS AND APPLICATIONS IN ENGINEERING Brain Tumor Detection Using Transfer Learning with Dimensionality Reduction Method," *Original Research Paper International Journal of Intelligent Systems and Applications in Engineering IJISAE*, vol. 2022, no. 2, pp. 201–206, doi: 10.18201/ijisae.

[5]   M. O. Khairandish, M. Sharma, V. Jain, J. M. Chatterjee, and N. Z. Jhanjhi, "A Hybrid CNN-SVM Threshold Segmentation Approach for Tumor Detection and Classification of MRI Brain Images," *IRBM*, vol. 43, no. 4, pp. 290–299, Aug. 2022, doi: 10.1016/j.irbm.2021.06.003.

[6]   H. Kibriya, R. Amin, J. Kim, M. Nawaz, and R. Gantassi, "A Novel Approach for Brain Tumor Classification Using an Ensemble of Deep and Hand-Crafted Features," *Sensors*, vol. 23, no. 10, May 2023, doi: 10.3390/s23104693.

[7]   W. Widhiarso, Y. Yohannes, and C. Prakarsah, "Brain Tumor Classification Using Gray Level Co-occurrence Matrix and Convolutional Neural Network," *IJEIS (Indonesian Journal of Electronics and Instrumentation Systems)*, vol. 8, no. 2, p. 179, Oct. 2018, doi: 10.22146/ijeis.34713.

[8]   S. Khawaldeh, U. Pervaiz, A. Rafiq, and R. Alkhawaldeh, "Noninvasive Grading of Glioma Tumor Using Magnetic Resonance Imaging with Convolutional Neural Networks," *Applied Sciences*, vol. 8, no. 1, p. 27, Dec. 2017, doi: 10.3390/app8010027.

[9] P. K. Ramtekkar, A. Pandey, and M. K. Pawar, "Innovative brain tumor detection using optimized deep learning techniques," *International Journal of System Assurance Engineering and Management*, vol. 14, no. 1, pp. 459–473, Feb. 2023, doi: 10.1007/s13198-022-01819-7.

[10] D. Rammurthy and P. K. Mahesh, "Whale Harris hawks optimization based deep learning classifier for brain tumor detection using MRI images," *Journal of King Saud University - Computer and Information Sciences*, vol. 34, no. 6, pp. 3259–3272, Jun. 2022, doi: 10.1016/j.jksuci.2020.08.006.

[11] S. Maqsood, R. Damaševičius, and R. Maskeliūnas, "Multi-Modal Brain Tumor Detection Using Deep Neural Network and Multiclass SVM," *Medicina (Lithuania)*, vol. 58, no. 8, Aug. 2022, doi: 10.3390/medicina58081090.

[12] M. Sajjad, S. Khan, K. Muhammad, W. Wu, A. Ullah, and S. W. Baik, "Multi-grade brain tumor classification using deep CNN with extensive data augmentation," *J Comput Sci*, vol. 30, pp. 174–182, Jan. 2019, doi: 10.1016/j.jocs.2018.12.003.

[13] A. Younis, L. Qiang, C. O. Nyatega, M. J. Adamu, and H. B. Kawuwa, "Brain Tumor Analysis Using Deep Learning and VGG-16 Ensembling Learning Approaches," *Applied Sciences (Switzerland)*, vol. 12, no. 14, Jul. 2022, doi: 10.3390/app12147282.

[14] A. Gumaei, M. M. Hassan, M. R. Hassan, A. Alelaiwi, and G. Fortino, "A Hybrid Feature Extraction Method With Regularized Extreme Learning Machine for Brain Tumor Classification," *IEEE Access*, vol. 7, pp. 36266–36273, 2019, doi: 10.1109/ACCESS.2019.2904145.

[15] F. S. Baji, S. B. Abdullah, and F. S. Abdulsattar, "K-mean clustering and local binary pattern techniques for automatic brain tumor detection," *Bulletin of Electrical Engineering and Informatics*, vol. 12, no. 3, pp. 1586–1594, Jun. 2023, doi: 10.11591/eei.v12i3.4404.

[16] A. K. Sharma, A. Nandal, A. Dhaka, D. Koundal, D. C. Bogatinoska, and H. Alyami, "Enhanced Watershed Segmentation Algorithm-Based Modified ResNet50 Model for Brain Tumor Detection," *Biomed Res Int*, vol. 2022, 2022, doi: 10.1155/2022/7348344.

[17] R. Vankdothu, M. A. Hameed, and H. Fatima, "A Brain Tumor Identification and Classification Using Deep Learning based on CNN-LSTM Method," *Computers and Electrical Engineering*, vol. 101, Jul. 2022, doi: 10.1016/j.compeleceng.2022.107960.

[18] A. H. Khan *et al.*, "Intelligent Model for Brain Tumor Identification Using Deep Learning," *Applied Computational Intelligence and Soft Computing*, vol. 2022, 2022, doi: 10.1155/2022/8104054.

[19] H. A. Shah, F. Saeed, S. Yun, J. H. Park, A. Paul, and J. M. Kang, "A Robust Approach for Brain Tumor Detection in Magnetic Resonance Images Using Finetuned EfficientNet," *IEEE Access*, vol. 10, pp. 65426–65438, 2022, doi: 10.1109/ACCESS.2022.3184113.

[20] N. M. Dipu, S. A. Shohan, and K. M. A. Salam, "Deep Learning Based Brain Tumor Detection and Classification," in *2021 International Conference on Intelligent Technologies, CONIT 2021*, Institute of Electrical and Electronics Engineers Inc., Jun. 2021. doi: 10.1109/CONIT51480.2021.9498384.

[21] M. I. Sharif, J. P. Li, J. Amin, and A. Sharif, "An improved framework for brain tumor analysis using MRI based on YOLOv2 and convolutional neural network," *Complex and Intelligent Systems*, vol. 7, no. 4, pp. 2023–2036, Aug. 2021, doi: 10.1007/s40747-021-00310-3.

[22] H. M. Ünver and E. Ayan, "Skin Lesion Segmentation in Dermoscopic Images with Combination of YOLO and GrabCut Algorithm," *Diagnostics*, vol. 9, no. 3, p. 72, Jul. 2019, doi: 10.3390/diagnostics9030072.

[23] P. Gao, J. Lu, H. Li, R. Mottaghi, and A. Kembhavi, "Container: Context Aggregation Network," Jun. 2021, [Online]. Available: http://arxiv.org/abs/2106.01401

[24] P. Dollár, M. Singh, and R. Girshick, "Fast and Accurate Model Scaling." [Online]. Available: https://github.com/facebookresearch/pycls

[25] P. Kumar, A. Vasu, J. Gabriel, J. Zhu, O. Tuzel, and A. Ranjan Apple, "MobileOne: An Improved One millisecond Mobile Backbone."

[26] K. Liu, Q. Sun, D. Sun, M. Yang, and N. Wang, "Underwater target detection based on improved YOLOv7." [Online]. Available: https://github.com/NZWANG/YOLOV7-AC.

[27] X. Ding, X. Zhang, N. Ma, J. Han, G. Ding, and J. Sun, "RepVGG: Making VGG-style ConvNets Great Again." [Online]. Available: https://github.

[28] J. Redmon and A. Farhadi, "YOLO9000: Better, Faster, Stronger." [Online]. Available: http://pjreddie.com/yolo9000/

[29] J. Redmon and A. Farhadi, "YOLOv3: An Incremental Improvement," Apr. 2018, [Online]. Available: http://arxiv.org/abs/1804.02767

[30] P. Henderson and V. Ferrari, "End-to-end training of object class detectors for mean average precision," Jul. 2016, [Online]. Available: http://arxiv.org/abs/1607.03476

[31] H. M. Ünver and E. Ayan, "Skin lesion segmentation in dermoscopic images with combination of yolo and grabcut algorithm," *Diagnostics*, vol. 9, no. 3, Sep. 2019, doi:

10.3390/diagnostics9030072.

[32] A. Bochkovskiy, C.-Y. Wang, and H.-Y. M. Liao, "YOLOv4: Optimal Speed and Accuracy of Object Detection," Apr. 2020, [Online]. Available: http://arxiv.org/abs/2004.10934

[33] E. Avşar and K. Salçin, "Detection and classification of brain tumours from MRI images using faster R-CNN," *Tehnički glasnik*, vol. 13, no. 4, pp. 337–342, Dec. 2019, doi: 10.31803/tg-20190712095507.

[34] Sri Eshwar College of Engineering and Institute of Electrical and Electronics Engineers, *2020 6th International Conference on Advanced Computing and Communication Systems (ICACCS).*

[35] N. M. Dipu, S. A. Shohan, and K. M. A. Salam, "Deep Learning Based Brain Tumor Detection and Classification," in *2021 International Conference on Intelligent Technologies, CONIT 2021*, Institute of Electrical and Electronics Engineers Inc., Jun. 2021. doi: 10.1109/CONIT51480.2021.9498384.

[36] Anaya-Isaza, Andrés, and Leonel Mera-Jiménez. "Data augmentation and transfer learning for brain tumor detection in magnetic resonance imaging." IEEE Access 10 (2022): 23217-23233.

[37] Walker David, A., et al. "Brain and spinal tumors of childhood." (2004): 3-531.

[38] Alan, Nima, John C. Flickinger, and Peter Carlos Gerszten. "Spinal meningioma." Adult CNS Radiation Oncology: Principles and Practice (2018): 117-125.

[39] M. E. Molitch, "Diagnosis and treatment of pituitary adenomas: a review," Jama, vol. 317, no. 5, pp. 516-524, 2017.

[40] DeAngelis, Lisa M. "Brain tumors." New England journal of medicine 344.2 (2001): 114-123.

[41] Alsaif, Haitham, et al. "A novel data augmentation-based brain tumor detection using convolutional neural network." Applied Sciences 12.8 (2022): 3773.

[42] Ullah, Naeem, et al. "An effective approach to detect and identify brain tumors using transfer learning." Applied Sciences 12.11 (2022): 5645.

[43] Rajinikanth, Venkatesan, et al. "A customized VGG19 network with concatenation of deep and handcrafted features for brain tumor detection." Applied Sciences 10.10 (2020): 3429.